

**THEORETICAL MODELLING OF SOLAR STILL FOR  
WATER DISTILLATION IN YOLA NIGERIA**

**ALKASIM, ABUBAKAR**

**JANUARY, 2013**

**THEORETICAL MODELLING OF SOLAR STILL FOR WATER  
DISTILLATION IN YOLA NIGERIA**

**By**

**ALKASIM, ABUBAKAR**

**(Ph.D/PH/07/ 0138)**

**A THESIS SUBMITTED TO THE SCHOOL OF POSTGRADUATE STUDIES,  
MODIBBO ADAMA UNIVERSITY OF TECHNOLOGY, YOLA IN PARTIAL  
FULFILMENT FOR THE REQUIREMENTS OF THE AWARD OF DOCTOR  
OF PHILOSOPHY IN ENERGY PHYSICS OF THE DEPARTMENT OF  
PHYSICS SCHOOL OF PURE AND APPLIED SCIENCES.**

**JANUARY, 2013**

**DECLARATION**

I hereby declare that this thesis was written by me and it is a record of my own research work. It has not been presented before in any previous application for a higher degree. All references cited have been duly acknowledged.

---

**Abubakar Alkasim**

---

**Date**

**APPROVAL**

This thesis entitled **THEORETICAL MODELLING OF SOLAR STILL FOR WATER DISTILLATION IN YOLA NIGERIA** by Abubakar Alkasim

(Ph.D/PH/07/0138) meets the regulations governing the award of Doctor of Philosophy (Ph.D) in Energy Physics of the Modibbo Adama University of Technology, Yola and is approved for its contribution to knowledge and literary presentation.

---

Major Supervisor:

Dr. Adam Usman

---

Date

---

Co-Supervisor:

Professor J.C. Ododo

---

Date

---

Internal Examiner:

Dr. A.D. Ahmed

---

Date

---

External Examiner:

Professor M.A.C. Chendo

---

Date

---

---

The Head of Department:

Date

Dr. J.B. Yerima

---

Dean School of Pure and Applied Sciences

Date

Professor M.M. Malgwi

---

Dean School of Postgraduate Studies

Date

Professor M.R. Odekunle

## **DEDICATION**

To the family of **Mallam Alkasim Salihu Ganye**

## **ACKNOWLEDGEMENT**

In the name of Allah the most Gracious the most Merciful. All praises and thanks are due to Allah the Lord of the World. This work will not have been a reality without the help of my able supervisors Dr. Adam Usman, who spent much time in going through the manuscripts of the work and offer constructive advice and Professor J.C. Ododo. I thank you sirs. My sincere appreciation goes to the University management of Modibbo Adama University of Technology, Yola (MAUTECH, Yola) for sponsoring me. I can say that the time allowed to me is positively utilized due to your full support. Thanks a lot.

My appreciations go to the entire staff of the Nigerian Environmental Climatic Observing Programm (NECOP), University of Nigeria Nsukka most especially the scientific Officer I, Engineer Najib Yusuf Galadanci as well as Engineer Nasiru Aliyu who were ever ready to attend to my need partaining the data logger and Yola station. Also to all staff of the Department of Physics in particular and the University at large. I appreciate your kindness and advice.

I will not forget the efforts of my wife, Rukaiyya Abdullahi, my mother, (Hajiya) Aisha (*Adda Azumi*) and my Brother Mudassiru Alkasim my children

Fatima, Abdulaziz, Abdulrahman and little Alkasim for their moral support and prayers during the course of this reseach.

I acknowledge my course mate and colleague Mr. Pascal Timtere for his friendly support and advice. Same goes to my big brother mallam Chiroma Tahir HOD Islamic Studies Department F.C.E. Yola. I profoundly thank and appreciate the support of my friends: Mallam Mohammed T. Zakari, of Survey Department Adamawa State Polytechnic, Yola, Mallam Abdullahi S. Bashir, of Information Technology Department, MAUTECH, Yola, Mallam Shatima of State Fire service division, Yola and Mallam Yusuf Sa'ad of University clinic, MAUTECH, Yola.

Lastly, I appreciate the contributions of friends, relatives and well wishers whose names did not appear here, but contributed in one way or the other towards the success of this programme.

Thank you and God Bless.

### ABSTRACT

A theoretical model was developed for a static flat plate solar distiller used for distillation of water in Yola (9.23°N, 13°E) North-Eastern Nigeria. The modelling was done on the solar still efficiency,  $\eta$  based on the view factors  $F_1$ ,  $F_2$ , for the respective **top** and **side-wall** correction factors. The modeled efficiency  $\eta$ , is

$$\eta = \frac{h_{ew} F_1 h_2}{h_1 + F_1 h_2} \frac{1}{U_L} \times \left[ (\alpha \tau)_{eff} (1 - e^{-a\Delta t}) + U_L \frac{(T_{w0} - T_a)}{H_s} e^{-a\Delta t} \right].$$

The model could be extended to work at every other point in the Sub Saharan countries with relative climatic condition. From the simulated model, the rate of production of fresh water is calculated as a function of different meterological parameters and the solar still specifications. A solar still was then constructed to validate and test the model. The results of the cumulative yield based on the simulated model are compared with that of the experiment at an initial water depth of 1.0 cm. There is good agreement between the two with a very little under estimation experimentally (average  $R^2 = 0.999$  for the theoretical model and  $R^2 = 0.998$  for the experiment). The daily distillate was 1.5 litres at an initial water depth of 3.0 cm and 3.3 litres at an initial water depth of 0.5 cm. A maximum average efficiency of 28% was obtained which was an improvement over the 26% and 25% obtained by some earlier researchers located at

other regions. The comparison between the simulated cumulative yield of the present model and that of Tiwari (2002) reveals that the present model results are more closer to the experimental result in Yola with a deviation of only 1.42% (21ml) for the present model and 4.79% (71ml) for the later from the observed values. The model was tested against data from Makurdi, Jos and Abuja and the result show that the  $R^2$  fit for the efficiency is 0.945, 0.996 and 0.626 respectively.

<b>TABLE OF CONTENTS</b>										<b>Page</b>
COVER PAGE	-	-	-	-	-	-	-	-	-	i
TITLE PAGE	-	-	-	-	-	-	-	-	-	ii
DECLARATION	-	-	-	-	-	-	-	-	-	iii
APPROVAL	-	-	-	-	-	-	-	-	-	iv
DEDICATION	-	-	-	-	-	-	-	-	-	v
ACKNOWLEDGEMENT	-	-	-	-	-	-	-	-	-	vi
ABSTRACT	-	-	-	-	-	-	-	-	-	vii
TABLE OF CONTENTS	-	-	-	-	-	-	-	-	-	viii
LIST OF TABLES	-	-	-	-	-	-	-	-	-	xii
LIST OF FIGURES	-	-	-	-	-	-	-	-	-	xiii
LIST OF PLATES	-	-	-	-	-	-	-	-	-	xix
LIST OF APPENDICES	-	-	-	-	-	-	-	-	-	xv
<b>CHAPTER ONE: INTRODUCTION</b>	-	-	-	-	-	-	-	-	-	1
1.1 Background of the Study	-	-	-	-	-	-	-	-	-	1
1.2 Statement of the Problem	-	-	-	-	-	-	-	-	-	3
1.3 Aim and Objectives	-	-	-	-	-	-	-	-	-	4
1.4 The Site of the Study	-	-	-	-	-	-	-	-	-	4
1.5 Significance of the Study	-	-	-	-	-	-	-	-	-	5
1.6 Feasibility of the Study	-	-	-	-	-	-	-	-	-	5
<b>CHAPTER TWO: LITERATURE REVIEW-</b>	-	-	-	-	-	-	-	-	-	6
2.1 Introduction	-	-	-	-	-	-	-	-	-	6
2.2 The solar radiation	-	-	-	-	-	-	-	-	-	6
2.2.1 Beam (Direct) Radiation ( $I_b$ )	-	-	-	-	-	-	-	-	-	7
2.2.2 Diffuse Radiation ( $I_d$ )	-	-	-	-	-	-	-	-	-	7
2.2.3 Total Solar (Global) Radiation ( $I$ )	-	-	-	-	-	-	-	-	-	7
2.3 Availability of Solar Radiation on an Inclined Surface	-	-	-	-	-	-	-	-	-	8
2.4 Definition of Terms Used in Solar Energy Applications	-	-	-	-	-	-	-	-	-	10
2.5 History of Solar stills	-	-	-	-	-	-	-	-	-	11
2.6 Effect of various parameters on solar still	-	-	-	-	-	-	-	-	-	12
2.6.1 Effect of Wind Velocity	-	-	-	-	-	-	-	-	-	13
2.6.2 Effect of Ambient Temperature	-	-	-	-	-	-	-	-	-	13
2.6.3 Effect of Solar Radiation and Loss Coefficient	-	-	-	-	-	-	-	-	-	13

2.6.4	Effect of Double-glass Cover and cover Inclination	-	-	-	-	-	-	14
2.6.5	Effect of Salt Concentration	-	-	-	-	-	-	14
2.6.6	Effect of Thermal Capacity and Water Depth	-	-	-	-	-	-	14
2.6.7	Effect of Charcoal Pieces on the Still Performance	-	-	-	-	-	-	15
2.6.8	Effect of the Formation of Algae and Mineral Layers on Water and Basin liner	-	-	-	-	-	-	15
2.7	Various Designs of Solar Still-	-	-	-	-	-	-	16
2.7.1	Single Slope Solar Still with Condenser	-	-	-	-	-	-	16
2.7.2	Hybrid Single Slope Still	-	-	-	-	-	-	17
2.7.3	Reverse Absorber Solar Still	-	-	-	-	-	-	18
2.7.4	Multi-wick Solar Still	-	-	-	-	-	-	18
2.7.5	Conical Solar Still	-	-	-	-	-	-	19
2.7.6	Active Single Slope Solar Still	-	-	-	-	-	-	20
2.8	Modelling as a tool for Physics Research	-	-	-	-	-	-	22
2.9	Review of Some Relevant Researches on Solar Still Modelling	-	-	-	-	-	-	23
2.10	Present Works on Solar Stills	-	-	-	-	-	-	26
	<b>CHAPTER THREE: MATERIALS AND METHODS</b>	-	-	-	-	-	-	28
3.1	Introduction	-	-	-	-	-	-	28
3.2	Theories on Solar Water Distillation	-	-	-	-	-	-	28
3.3	Thermal Analysis and the Energy Balances	-	-	-	-	-	-	30
3.3.1	The Energy Balances	-	-	-	-	-	-	30
3.4	The Heat Transfers	-	-	-	-	-	-	32
3.5	The External Heat Transfer	-	-	-	-	-	-	32
3.5.1	Top Loss Coefficient	-	-	-	-	-	-	32
3.6	Theoretical Modelling-	-	-	-	-	-	-	36
3.6.1	Bottom and Side Loss Coefficient	-	-	-	-	-	-	37
3.7	The Internal Heat Transfer	-	-	-	-	-	-	38
3.7.1	Radiative Loss Coefficient	-	-	-	-	-	-	39
3.7.2	Convective Loss Coefficient	-	-	-	-	-	-	40
3.7.3	Evaporative Loss Coefficient	-	-	-	-	-	-	42
3.8	The Thermal Modelling of the Still	-	-	-	-	-	-	44
3.8.1	Inner and outer Surfaces of the Glass cover	-	-	-	-	-	-	44
3.8.1.1	Inner side of the glass cover	-	-	-	-	-	-	44

3.8.1.2	Outer side of the glass cover	-	-	-	-	-	-	-	45
3.8.2	The basin liner-	-	-	-	-	-	-	-	46
3.8.3	The Water Mass	-	-	-	-	-	-	-	46
3.9	The Approximate Solution for the New Water Temperature, $T_w$	-	-	-	-	-	-	-	49
3.10	Steps in Solving the Theoretical Model	-	-	-	-	-	-	-	51
3.11	Materials and Construction	-	-	-	-	-	-	-	54
3.11.1	Materials for the Experiment	-	-	-	-	-	-	-	54
3.11.2	Construction Materials	-	-	-	-	-	-	-	54
3.11.3	The Construction Procedure	-	-	-	-	-	-	-	54
3.11.4	The Method of Experimental Observation	-	-	-	-	-	-	-	56
3.12	Operational Frame Work	-	-	-	-	-	-	-	57
3.13	Method of Data Collection	-	-	-	-	-	-	-	57
3.13.1	Theoretical Data Generation	-	-	-	-	-	-	-	57
3.13.2	Data Acquisition System	-	-	-	-	-	-	-	57
3.13.3	Data Acquisition Program	-	-	-	-	-	-	-	58
3.13.4	Sensors-	-	-	-	-	-	-	-	59
	<b>CHAPTER FOUR: RESULTS</b>	-	-	-	-	-	-	-	61
4.1	Introduction	-	-	-	-	-	-	-	61
4.2	Results-	-	-	-	-	-	-	-	61
4.2.1	The Water Quality Test Results	-	-	-	-	-	-	-	61
4.3.2	The Theoretical Modelling Results	-	-	-	-	-	-	-	64
4.3.3	The Experimental Results	-	-	-	-	-	-	-	83
	<b>CHAPTER FIVE: DISCUSSION</b>	-	-	-	-	-	-	-	142
5.1	Introduction	-	-	-	-	-	-	-	142
5.2	Discussions	-	-	-	-	-	-	-	142
5.3	The Discussions on the Correlation	-	-	-	-	-	-	-	144
5.3.1	The Dry Day Correlation	-	-	-	-	-	-	-	144
5.3.2	Wet day correlation	-	-	-	-	-	-	-	145
	<b>CHAPTER SIX: SUMMARY, CONCLUSION &amp; RECOMMENDATION</b>	-	-	-	-	-	-	-	148
6.1	Introduction	-	-	-	-	-	-	-	148
6.2	Summary and Conclusion	-	-	-	-	-	-	-	148
6.3	Contribution to Knowledge	-	-	-	-	-	-	-	149
6.4	Recommendation	-	-	-	-	-	-	-	149

LIST OF REFERENCES	-	-	-	-	-	-	-	150
APPENDICES	-	-	-	-	-	-	-	157

## LIST OF TABLES

<b>Table</b>	<b>Title</b>	<b>Page</b>
Table 3.1	Heat and Mass Transfer Classification in conv. Solar Still -	32
Table 3.2	Value of Grashof no.( $Gr$ ) for different average spacing ( $X_I$ )	41
Table 3.3	Value of $C$ and $n$ for different Grashof number ranges - -	42
Table 3.4	Sensors Used in Data Acquisition & Generation - -	60
Table 4.1	Results of the Water Quality Test - - - -	62
Table 4.2	The comparison between the water quality of the constructed distiller and a standard electronic distiller - - - -	63
Table 4.3	The distiller specification - - - - -	64
Table 4.4a	The Theoretically Generated Data Using the Modeled Equations for a dry day in dry season - - - - -	65
Table 4.4b	The Theoretically Generated Data Using the Modeled Equations for a wet day in a wet season - - - - -	74
Table 4.5	The experimental results at initial water depth, $L = 0.5$ cm -	83
Table 4.6	The experimental results at initial water depth, $L = 1.0$ cm -	86
Table 4.7	The experimental results at initial water depth, $L = 1.5$ cm -	88
Table 4.8	The experimental results at initial water depth, $L = 2.0$ cm -	90
Table 4.9	The experimental results at initial water depth, $L = 2.5$ cm -	92
Table 4.10	The experimental results at initial water depth, $L = 3.0$ cm -	94
Table 4.11	Comparison between present work and Tiwari 2002 - -	96

## LIST OF FIGURES

<b>Figure</b>	<b>Title</b>	<b>Page</b>
Figure 2.1	Floating Solar Still, Designated for Emergency... - -	11
Figure 2.2	The Effect of Water Depth on Daily Yield - - -	15
Figure 2.3	Single Slope Solar Still with Condenser - - -	17
Figure 2.4	Hybrid Solar Distillation System - - -	17
Figure 2.5	Schematic View of Reverse Absorber Solar Still - -	18
Figure 2.6	Cross-sectional view of Multi-wick solar still - -	19
Figure 2.7	Schematic view of a conical solar still- - -	20
Figure 2.8	A schematic view of active solar still with single collector -	21
Figure 2.9	A Schematic view of active solar still with number of collectors	22
Figure 3.1	A typical single slope conventional solar still - -	28
Figure 3.2	A typical single slope basin solar still: showing energy balances	30
Figure 3.5	Flow chart for the distiller yield computation- - -	53
Figure 3.4	Sectional view of the distiller unit (not mounted) - -	55
Figure 3.5	The experimental set up of the solar still used (mounted) -	56
Figure 3.6	Schematic Diagram of the data acquisition system - -	58
Figure 4.1a	Monthly average solar radiation and ambient temp. for Yola	98
Figure 4.1b	Monthly average relative humidity and wind speed for Yola-	98
Figure 4.2	The variation of solar rad. with time for Yola in dry season	99
Figure 4.3	The variation of solar rad. with time for Yola in the wet season	100
Figure 4.4	The variation of cum. yield with time for Yola in dry season-	101
Figure 4.5	The variation of cumulative yield with the day time for Yola in wet season - - - - -	102
Figure 4.6	The variation of the Distiller efficiency with time of the day in dry season - - - - -	103
Figure 4.7	The variation of the Distiller efficiency with time of the day in wet season - - - - -	104
Figure 4.8	The comparison between the three distiller variables: ambient temperature., water temperature and glass cover temperature with time for Yola in the dry season - - - -	105

Figure 4.9	The comparison between the three distiller variables: ambient temperature., water temperature and glass cover temperature with time for Yola in the wet season - - -	106
Figure 4.10	The comparison between the relative humidity and the efficiency with time of the day for Yola in dry season - - -	107
Figure 4.11	The comparison between the relative humidity and the efficiency with time of the day for Yola in wet season - - -	108
Figure 4.12	The comparison between the distiller efficiency and wind velocity with time of the day for Yola in wet season - - -	109
Figure 4.13	The comparison between the distiller efficiency and wind velocity with time of the day for Yola in dry season - - -	110
Figure 4.14	The comparison between the distiller cummulative yield and wind velocity with time of the day for Yola in dry season - -	111
Figure 4.15	The comparison between the distiller cummulative yield and wind velocity with time of the day for Yola in wet season - -	112
Figure 4.16a	The correlation between efficiency and $H_s$ on 12/11/09 -	113
Figure 4.16b	The correlation between efficiency and $v$ on 12/11/09 -	113
Figure 4.16c	The correlation between efficiency and R.H on 12/11/09 -	114
Figure 4.16d	The correlation between efficiency and $T_a$ on 12/11/09 -	114
Figure 4.17a	The correlation between efficiency and $H_s$ on 1/08/09 -	115
Figure 4.17b	The correlation between efficiency and $T_a$ on 1/08/09 -	115
Figure 4.17c	The correlation between efficiency and R.H on 1/08/09 -	116
Figure 4.17d	The correlation between efficiency and $v$ on 1/08/09 -	116
Figure 4.18	The variation of the three distiller variables: $T_a$ , $T_w$ and $T_g$ at 0.5cm initial water depth experimentally with time - - -	117
Figure 4.19	The variation of the three distiller variables: $T_a$ , $T_w$ and $T_g$ at 1.0cm initial water depth experimentally with time - - -	118
Figure 4.20	The variation of the three distiller variables: $T_a$ , $T_w$ and $T_g$ at 1.5cm initial water depth experimentally with time - - -	119
Figure 4.21	The variation of the three distiller variables: $T_a$ , $T_w$ and $T_g$ at 2.0 cm initial water depth experimentally with time - - -	120
Figure 4.22	The variation of the three distiller variables: $T_a$ , $T_w$ and $T_g$ at 2.5 cm initial water depth experimentally with time - - -	121

Figure 4.23	The variation of the three distiller variables: $T_a$ , $T_w$ and $T_g$ at 3.0 cm initial water depth experimentally with time - - -	122
Figure 4.24	The variation of the distiller cumulative yield with time at various initial water depths- - - - -	123
Figure 4.25	Comparison of the theoretical and the experimental distiller cumulative yield on 25 July, 2011 for a day - - -	124
Figure 4.26	The corolative comparison between the theoretical and experimental distiller cumulative yield , 2011 for a complete day (24 hrs) as from 7 am to 7 am the next day - - - - -	125
Figure 4.27	The comparison of the present model with the Tiwari 2002 -	126
Figure 4.28	Variation of the Distiller yield and efficiency in Makurdi -	127
Figure 4.29	Variation of the Distiller yield and efficiency in Jos - -	128
Figure 4.30	Variation of the Distiller yield and efficiency in Abuja -	129

## LIST OF PLATES

<b>Plate</b>	<b>Title</b>	<b>Page</b>
Plate I	Painting the aluminum box with black paint - -	181
Plate II	Lagging the wooden box with cotton wool - -	182
Plate III	The metal box fitted into the lagged wooding box -	183
Plate IV	The complete metal frame- - - -	184
Plate V	The complete set up (front view) - - -	185
Plate VI	The complete set up (back view) - - -	186
Plate VII	The complete set up (right side view)- - -	187
Plate VIII	The complete set up (left side view) - - -	188
Plate IX	The student on site taking some readings - -	189
Plate X	The student on site recording the obtained values -	190
Plate XI	The main supervisor on site observing the results -	191
Plate XII	The data logger used for storing data - - -	192
Plate XIII	The complete set up for experimental recording -	193

## LIST OF APPENDICES

	<b>Title</b>	<b>Page</b>
APPENDIX A	Nomenclature - - - - -	177
APPENDIX B	Plates display of the Life distiller construction stages	181
APPENDIX C	Cost of constructing a prototype solar still in Yola -	194
APPENDIX D	The location of the Nigerian State capitals on the globe	196
APPENDIX E	NECOP Yola Station's daily average data record for one year from December, 2010 to November, 2011- -	198
APPENDIX F	NECOP Yola Data record for three consecutive days in dry season: 1/1/2011 to 3/1/2011- - -	219
APPENDIX G	NECOP Yola Data record for three consecutive days in wet season: 27/7/2011 to 29/7/2011 - - -	271

# CHAPTER ONE

## INTRODUCTION

### 1.1 Background of the Study

The population increase, economic development, in addition to global warming is creating a worldwide imbalance between supply and demand of fresh water. Providing adequate supply of fresh water indeed becomes the most serious problem facing the whole world on the onset of this century. The most likely sources of water are the great oceans, seas and, in some remote areas wells that need to be desalinated and or distilled before it can be used. Most of the conventional distillation plants use fossil fuels or electricity as their source of energy (Van and Bas 2004). However, in many rural locations in Nigeria, grid-connected electricity is either unavailable or, for most of the people, too expensive. Thus for such remote locations, distillation of water that employs motorised or electrical heating is not appropriate. The large initial and running cost of alternative fossil fuel powered distillers present such financial barriers that they are rarely adopted by rural people. Although a few other techniques are employed e.g. Multi-effect evaporation, multistage flash distillation, thin film distillation, reverse osmosis and electrolysis, they are energy intensive and the operating cost is high as well (Van Frassen and Bas 2004; Bogen and James 1988).

There are basically three ways by which local people distill/clean their drinking water in tropical countries. These are:

- Filtration: using sieve
- Decantation: the water is allowed to settle naturally and then decant carefully into a clean basin
- Chemically: using alum

Despite the rudimentary nature of the processes involved, these techniques still remain in common use.

The use of solar still which directly uses solar energy is well suited for this task. This becomes increasingly attractive with time on account of the rapid increase in price of crude oil and its possibility of extinction (Garba *et al*, 1996).

A solar still (Garg and Prakash 1997) essentially consists of a mass of water in a container, which is covered by a transparent cover and the interior surface of this

enclosure is coated black to absorb solar radiation entering through the condensation of water vapour. The cover is sloped on one side to enable the condensation to trickle into a channel. The whole enclosure is insulated to minimise heat losses from the sides and the bottom surface.

Solar distillation (Mona *et al* 2002, Bemporad 1995, Harpreet and Kwatra 1996 and Kaabi and Smakdji 2007) represents a most attractive and simple technique among other distillation processes which suits a small-scale unit. It is environmentally friendly, of simple maintenance and technology and it is appropriate to developing countries (like Nigeria) with abundant solar radiation. It is necessary therefore to search for solar stills which could provide us with the necessary daily amount of fresh water, not forgetting the drought that has been prevailing in several areas of Africa for the last two decades (Sampathkumar *et al* 2010, Omar 2011 and Masoud *et al* 2010).

Distilled water is required for a number of uses such as institutions for laboratory experiments, health care centres, motor vehicle batteries, industrial and commercial organisations, aside the pressing need for drinking.

Modelling is of central importance in many scientific contexts. The centrality of models such as the Billiard ball model of a gas, the Bohr model of atom, the MIT bag model of the nucleon, the Gaussian-chain model of a polymer, the Lorenz model of the atmosphere, the Lotka-Volterra model of predator-prey interaction, the double helix model of DNA, the agent-based and evolutionary models in the social sciences, or the general equilibrium models of markets in their respective domains are cases in point (Bailer-Jones 2003, Frigg 2006, Giere 2004, Suárez 2004 and Van Frassen 2004). Scientists (Hudges 1997, Morgan 1999, Lloyd 1994, Brown 1991 and Reiss 2003) spend a great deal of time building, testing, comparing and reversing models, and much journal spaces are dedicated to introducing, applying and interpreting these valuable tools. In short, modelling is one of the principal instruments of modern science.

Philosophers are acknowledging the importance of models with increasing attraction and are probing the assorted roles that models play in scientific practice. The results have been an incredible proliferation of model-types in the philosophical literature (Ismo 2006; Asyegul and Salahattin 2010). Probing models, phenomenological models, computational models, developmental models, explanatory models, impoverished models, testing models, idealised models,

theoretical models, scale models, imaginary models, mathematical models, substitute models, iconic models, formal models, analogue models and instrumental models are some of the notions that are used to categorize models. These notions pertain to different problems that arise in connection with the models. Models are used to: learn the experiments, represent functions of a design piece, relate theories to the experiments and predict, explain and solve the problems of the laws of nature.

Models, (Van Frassen 2004, Bogen 1988) can perform two fundamentally different representational functions. On one hand, a model can be a representation of selected part of the world (target system), depending on the nature of the target. Such models are either models of phenomena or models of data. On the other hand, a model can represent a theory in the sense that it interprets the laws and axioms of that theory.

In this research, a theoretical model was developed for a simple static flat plate solar still (for simplicity) in Yola (9.23°N, 23°E) even though there are many models investigated. One was constructed using the locally available materials to test the viability of the model so developed. From the different data collected, many solar still parameters were obtained. The parameters are:- the quantity of the distillate produced per day, the thermal efficiency of the still, the rate of the distillate produced per small time interval, the effect of ambient temperature, relative humidity, wind speed and daily solar radiation on the still performance and the effect of initial water depth also on the still performance.

## **1.2 Statement of the Problem**

Some scientists like Mowla and Karimi (1995), Bachir (2002), Tiwari (2002) and Kaabi and Smakdji (2007), recently carried out an investigation on solar stills. They developed theoretical models on the stills which give the efficiency and the amount of the distillate produced daily using the solar insolation in Iran, Algeria and India respectively. The theoretical model goes fairly well with the designed solar stills in the area with little discrepancy. It was found out that their studies were limited to:

- (a) only the regions mentioned above
- (b) they used an angle of glass inclination not equal to the latitudes of the regions
- (c) some use the time range from 7 a.m – 4 p.m only
- (d) they ignored the side wall and top cover correction factor.

In this research, we intended to develop a model in Yola, North-Eastern Nigeria (Latitude 9.23<sup>0</sup>N, Longitude 13<sup>0</sup>E) which takes care of all the predicaments stated above and which could be as well extended to other parts of the country.

### **1.3 Aim and Objectives**

The aim of this work is to develop a theoretical model for a single plate static solar still here in Yola, North-Eastern Nigeria with a slopping angle equal to its latitude.

**The specific objectives are:**

- (a) To develop the theoretical model using available meteorological data for Yola-Nigeria (Latitude 9.23<sup>0</sup>N, Longitude 13<sup>0</sup>E) viz: solar insolation,  $H_s$ , ambient temperature,  $T_a$ , initial water temperature,  $T_{w0}$ , initial glass temperature,  $T_{g0}$  and wind speed,  $V$ , taking into consideration the side wall and top cover correction factors.
- (b) To construct a static, passive, single glass flat plate solar still sloped at an angle corresponding to the latitude of the study area, Yola using the available materials so as to test the model. Hence, compare the theoretically calculated distiller yield and efficiency based on the simulated model with the experimentally obtained results, extending the time range beyond 4:00 pm local time.
- (c) To study the effect of some meteorological data e.g. wind speed, solar radiation, ambient temperature and relative humidity on the distiller efficiency for a wet day and a dry day.

### **1.4 The site of the Study**

The site of this study is Yola (9.23<sup>0</sup>N, 13<sup>0</sup>E, altitude 186m above sea level) whose latitude, wind speed and other climatical parameters have been used in the data generation. The testing of the constructed solar still, data collection and analyses were done here in Yola. However, the mathematical model used in calculating the total distillate could be extended to some of the Nigerian Environmental Climatic Observing Program (NECOP) Stations mounted in other geopolitical zones of the country such as Jos (North- central), Makurdi and Abuja. The work is restricted to a single slope solar still.

## **1.5 Significance of the Study**

The significance of this work cannot be overemphasized owing to the pressing need for fresh/quality water and the abundance of solar radiation here in Nigeria. This study is important in

- (i) Still Modelling: addressing the problem of solar still models which don't take into cognisance the view factor parameters.
- (ii) Clean water provision: addressing the problems of clean water shortage which was the emphasis at every World Water Day celebration.
- (iii) Academics: can serve as a study material for further researches in the area of solar distillation for production of distilled water which is vital for domestic, industrial, clinical and research purposes.

## **1.6 Feasibility of the Study**

The research is feasible here in Yola, (9.23°N, 13°E) and can be easily completed. All the materials needed for the construction of the solar distiller are available and can be procured. For the solar still which can be constructed, the measuring instruments are available in the market. More so, the computers which shall be used for programming the theoretical model and analysing the data from the logger have been personally procured. The software to be used normally comes with the data logger which was installed by the NECOP in the Department of Physics, Modibbo Adama University of Technology, Yola.

## CHAPTER TWO

### LITERATURE REVIEW

#### 2.1 Introduction

In this chapter a general overview on the solar radiation was looked into. Then, various types of the solar distillers are reviewed, starting with the history of the development of such stills starting with a brief review on solar radiation. The research results obtained by other people in the area by employing different distiller designs are reported. Hence, the effects of various parameters like wind speed, ambient temperature, solar radiation e.t.c. on the solar still's performance are also reviewed. Modelling as a tool for scientific research was also reviewed.

#### 2.2 The Solar Radiation

Solar radiation originates from the sun as a result of the convective and radiative processes occurring inside the sun. The nature of this radiation is determined by the structure and characteristics of the sun itself (Meinel and Meinel 1977; Tiwari 2004 and Nwokoye 2006). The orientation of the earth's orbit around the sun is in such a way that the sun-earth distance varies only by 1.7%. Since the solar radiation outside the earth's atmosphere is nearly of fixed intensity, the radiant energy flux received per second by a surface of unit area held normal to the direction of the sun's rays at the mean sun-earth distance, outside the atmosphere, is practically constant throughout the year. This is termed solar constant,  $I_{sc}$  with a value of approximately  $1367 \text{ W/m}^2$ . However, this extraterrestrial radiation suffers variation due to the fact that the earth revolves around the sun not in a circular orbit but follows an elliptical path, with the sun as one focus. The intensity of this extraterrestrial radiation,  $I_{ext}$  measured in a plane normal to the radiation on the  $n$ th day of the year is given in terms of the solar constant  $I_{sc}$  as follows (Layi 1990; Duffie and Beckman 1991):

$$I_{ext} = I_{sc} \left[ 1.0 + 0.033 \cos \left( \frac{360n}{365} \right) \right] \quad (2.1)$$

where  $n$  is the number of the day with January 1<sup>st</sup> as  $n = 1$  and December, 31<sup>st</sup>, corresponds to  $n = 365$ .

From the view of terrestrial application of solar energy only radiations of wavelengths between  $0.29\mu\text{m}$  and  $2.3\mu\text{m}$  is significant (Tiwari 2002).

The solar radiation, through the atmosphere, reaching the earth's surface can be classified into (Meinel and Meinel 1977; Tiwari 2004 and Nwokoye 2006):- (i) Beam and (ii) diffused radiation and (iii) global radiation.

### **2.2.1 *Beam (Direct) Radiation ( $I_b$ )***

This is the solar radiation propagating along the line joining the receiving surface and the sun. The direct radiation is measured by an instrument called Pyrheliometer, an instrument with a small conical aperture slightly wider than the solid angle subtended by the solar disc. The instrument is normally mounted equatorially to follow the sun (Tiwari 2004 and Nwokoye 2006).

### **2.2.2 *Diffuse Radiation ( $I_d$ )***

This is the solar radiation scattered by aerosols, dust and molecules. It does not have a single direction. Diffused radiation is measured by an instrument called pyranometer. The instrument is fitted with a device that occults the beam radiation from the solar disk. There are two types of occulting devices (i) a circular disk 15 cm in diameter placed about 1m away from the sensor of the pyranometer. (ii) a shadow band mounted on an east-west axis which blocks off beam radiation and a small amount of radiation from reaching the sensor, which results in slightly lower readings of diffuse irradiance. A correction factor is normally applied to take care of this error (Tiwari 2004 and Nwokoye 2006).

### **2.2.3 *Total Solar (Global) Radiation ( $I$ )***

The total solar radiation is the sum of the beam and diffused radiation. It is sometimes referred to as insolation per unit time. Available global solar radiation on a horizontal surface can be measured directly using Pyranometer (Tiwari 2004 and Nwokoye 2006). Nevertheless, it is often desirable to know the individual levels of beam and diffuse radiation for purposes of solar energy system modelling, design, testing and application (Volker 2005, Fedalis and Bougriou 2010, and BenHalima *et al* 2012).

### 2.3 Availability of Solar Radiation on an Inclined Surface

Usually the global radiation (beam + diffused) together with the radiation reflected from the ground and surroundings falling on a horizontal surface are directly recorded. In cases where the data for the beam,  $I_b$  and diffused,  $I_d$  radiations are not available the following expressions (Layi 1990) are used

$$I_b = I_N \cos\theta_Z \quad (2.2)$$

and

$$I_d = \left(\frac{1}{3}\right)[I_{ext} - I_N] \cos\theta_Z \quad (2.3)$$

where  $\theta_Z$  is the zenith angle: an angle between sun's ray and the perpendicular line to the horizontal plane,  $I_{ext}$  is the extraterrestrial irradiance and  $I_N$  is the intensity of the beam radiation given as

$$I_N = I_{ext} \exp[-T_R / (0.9 + 9.4 \sin \alpha)], \quad \alpha = 90 - \theta_Z \quad (2.4)$$

where  $T_R$  is the turbidity factor, which for a cloudy condition,  $T_R = 10$ .

When the beam and diffused radiations are known for a horizontal surface, the formula for a surface of an arbitrary orientation (inclined surface) is given by Liu and Jordan as reported in (Tiwari 2002 and Nwokoye 2006) as

$$I_T = I_b R_b + I_d R_d + \rho_g R_r (I_b + I_d) \quad (2.5)$$

where  $R_b$  (= ratio of the flux of beam radiation incident on an inclined surface to that on horizontal);  $R_d$  (= ratio of the diffused radiation incident on an inclined surface to that on horizontal) and  $R_r$  (= the reflected component mainly from the ground and surroundings) are the conversion factors for the beam, diffused and reflected components respectively and  $\rho$  is the reflection coefficient of the ground (~ 0.2 and 0.6 for ordinary and snow covered ground respectively). The expressions for the conversion factors are as follows:

$$R_b = \frac{\cos\theta_i}{\cos\theta_H} \quad (2.6)$$

$$R_d = \frac{1 + \cos \beta}{2} \quad (2.7)$$

$$R_r = \left( \frac{1 - \cos \beta}{2} \right) \quad (2.8)$$

where  $\theta_i$  and  $\theta_H$  are the angles of incidence on inclined and horizontal surfaces respectively,  $\beta$  is the inclination of the plane.

Both the beam and diffused components of radiation suffers reflection from the ground and the surroundings. The variation of  $R_d$  and  $R_r$  with inclination,  $\beta$  for some specific values indicated that for  $\beta = 90^\circ$ ,  $R_d = R_r = 0.5$  (Masoud *et al* 2010). Thus indicating that half of diffuse and half of the reflected total radiation is received by vertical plane. For horizontal plane,  $R_d = 1$ ,  $\beta = 0$ ,  $R_r = 0$ , indicating that horizontal plane receives no reflected radiation.

The optimum tilt (inclination) of solar collector with respect to user is an important subject from application of thermal/electrical energy point of view. By utilizing maximum solar energy through the optimum tilt, we are able to harness the energy needed without much pollution to the environment. Optimum tilt can be achieved by using tracking systems either manually or automatically. It is normally done through (i) monthly based optimization (ii) seasonal based optimization.

It is possible to collect 40 % more solar energy by using a two-axis tracking system and it is estimated that in sunny climates, a flat-plate collector moved to face the sun twice a day can intercept nearly 95 % of the energy collected using a fully automatic solar tracking system (Ahmad and Tiwari 2009).

Generally, in the northern hemisphere, the optimum collector orientation is south facing ( $\gamma = 0$ ) and the optimum tilt depends upon the latitude and the day of the year. in winter months, the optimum tilt is greater (usually latitude  $+15^\circ$ ), whilst in summer months, the optimum tilt is less (usually latitude  $-15^\circ$ ). Based on this fact Ahmad and Tiwari (2009) conducted a research by setting up 30 stations in different parts of the world. The results of their research indicated that the annual based optimum tilt in each location is approximately equal to its latitude. The same result is reported by the works of Sampathkumar *et al*, (2010) in India.

## 2.4 Definition of Terms Used in Solar Energy Applications

**(i) Latitude ( $\phi$ ):** The latitude of a location is the angle made by the radial line joining the given location to the center of the earth, with its projection on the equatorial plane. It is positive for the northern hemisphere and negative for southern hemisphere.

**(ii) Declination ( $\delta$ ):** declination is defined as the angle between the line joining the centers of the sun and the earth and its projection on the equatorial plane. Its due to the rotation of the earth about an axis which makes an angle of  $66\frac{1}{2}^\circ$  with the plane of its rotation round the sun. The declination varies from a maximum value of  $23.45^\circ$  on June 21 to a minimum value of  $-23.45^\circ$  on December, 21. rotation. It may be calculated by the following relation (Cooper 1969, Tiwari 2002)

$$\delta = 23.5 \sin \left[ \frac{360}{365} \times (284 + n) \right] \quad (2.9)$$

where  $n$  is the day number of the year,  $n = 1$  for January 1.

**(iii) Hour angle ( $\omega$ ):** It is the angle through which the earth must be rotated to bring the meridian of the plane directly under the sun. In other words it is the angular displacement of the sun to the east or west of the local meridian, due to the rotation of the earth on its axis at  $15^\circ$  per hour. The hour angle is zero at solar noon, negative in the morning and positive in the afternoon. The expression for the hour angle is given as

$$\omega = (ST - 12) 15^\circ \quad (2.10)$$

**(iv) Irradiance ( $W/m^2$ ):** this is the rate at which radiant energy is incident on a surface, per unit area of the surface.

Irradiation or Radiant exposure ( $J/m^2$ ): this refers to the incident energy per unit area on a surface, found by integrating the irradiance over a specified time. The symbol  $H$  is used to denote insolation for a day (daily insolation) and  $I$  is used to denote insolation for an hour (hourly insolation). Both  $H$  and  $I$  can represent beam radiation, diffused radiation or total radiation and can be on surfaces of any orientation (Tiwari 2002).

**(v) Radiosity or Radiant Exitance ( $W/m^2$ ):** this is the rate at which radiant energy leaves a surface per unit area, by combined emission and transmission.

(vi) **Emissive Power or Radiant Self-exittance ( $W/m^2$ )**: this is the rate at which radiant energy leaves a surface per unit area, by emission only.

(vii) **Albedo**: this refers to the situation where by the earth reflects about 30% of the incoming solar radiation back to extraterrestrial region through the atmosphere.

## 2.5 History of Solar Stills

Solar distillation is used to supply small communities with fresh and distilled water, where clean drinking water is hardly obtained. Solar distillation has been used since many centuries ago. The Arab Alchemist was believed to have set up, in 1551, apparatus for water desalination (Malik *et al* 1982).

The first large conventional solar still appeared in 1872 near a town called Las Salinas Northern Chile. The model has been made up by Carlos Wilson, a Swedish engineer, with a glazed surface spread over an area measuring 5000 m<sup>2</sup>. The plant produces about 19 m<sup>3</sup>/day of fresh water. The still kept operating for nearly thirty (30) years, until 1910 when a pipeline was constructed to bring water from the Andes Mountains to Antofagasta owing to the rapid accumulation of salts in the basin which requires a regular cleaning of the still (Talbert *et al* 1970).

At the beginning of 1930's, Trifinov proposed a cylindrical still (Telkes 1945). Abbot in 1938, used cylindrical and parabolic reflectors, to concentrate solar rays and the overall is conveyed in tubes filled with water (Telkes 1945).

Maria Telkes, in 1945, discovered a new type of solar still called 'Spherical still' which was used by the American marines: about 200,000 of this model were used during the World War II.

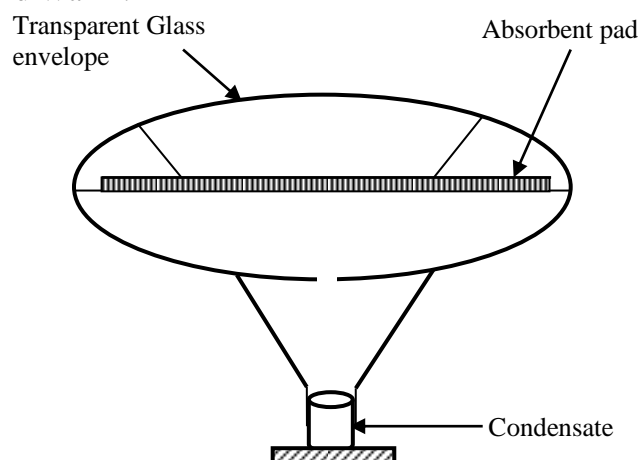


**Figure 2.1:** *Floating Solar Still, Designated for Emergency use in the Life Rafts, Schematic representation only (Source: Telkas 1945).*

The device consisted of an inflated transparent plastic envelop that would float in the sea, and which contained a black absorbent pad saturated with sea water. The sun shining through the upper part of the plastic envelop heated the absorbent pad and evaporated part of the sea water from it. Part of the vapour so formed condensed on the inner top surface of an envelop and was collected in a cup at the bottom. When the cup was full, the device was lifted out of the sea and the fresh water drained out of it. The absorbent pad has an area of about  $0.2 \text{ m}^2$ , and the device would produce nearly a litre of water on a clear day. Work on these devices practically ceased at the end of the war.

Cooper was the first person to propose a mathematical simulation in 1970s to analyse the efficiency of green-house solar still (Cooper 1969). Since 1970s, many other types of solar stills have been elaborated and studied, from which we can quote: multiple-effect solar still, steeped plate or steeped solar still, wick-type solar still or multiple-wick solar still and the combined solar still green house (Howe 1992).

Many countries have also utilized theoretical modelling to produce working solar stills. Examples are Algeria in 1963, (Savornin 1961), Australia in 1963 and 1967, (Delyannis 1968), Chile between 1969 and 1970, (Gomkele 1964), Greece between 1964 and 1973, (Delyannis 1968), India between 1957 and 1966, Tunisia in 1960 and U.S.A in 1952, (Howe and Thimat 1974).

Research and development efforts on the device reached a peak in the middle of 1960s, but decreased to a very low level by 1970. It was generally concluded that solar distillation using the device developed, produced fresh water at a cost greater than that of the water produced by desalination methods energized by fuels (Howe and Tleimat 1974). However, the experimental work done during the active period of the 1950s and 1960s gives an extensive body of experimental data. These allow for analytical basis for the design and prediction of the performance of conventional solar stills. However, the quality of the experimentally obtained distillate can be compared with that obtained from the electrical distiller.

## **2.6 Effect of Various Parameters On Solar Still**

The total yield of a solar still depends basically on the difference between the temperature of water ( $T_w$ ) in the basin and the temperature of the condensing glass cover ( $T_g$ ) in such a way that the higher the value of  $(T_w - T_g)$ , the greater the yeild.

Some researchers such as Satcunanathan and Deonarine (1973); Garba *et al* (1996) and Goyal and Tiwari (1999), investigated some of the parameters involved in solar distillation and their effect on the yield. The parameters and their effects are as follows:

### **2.6.1 Effect of Wind Velocity**

From the results of the experiments conducted by Cooper (1969), the output increases by 11.5% for average wind velocities ranging from 0 to 2.15 ms<sup>-1</sup>, while the increase is only 1.5% for average wind velocities ranging from 2.15 ms<sup>-1</sup> to 8.81 ms<sup>-1</sup>. Thus if the wind speed is too high, it has no significant effect on the distillation rate.

The wind over the glass cover causes faster evaporation from it resulting in a fall in the temperature, thus increasing the yeild from the solar still for larger water depth. However, for smaller water depth the wind has no effect on the output of the still. Even for larger water depth, wind velocity above 5 ms<sup>-1</sup> has not much effect on the yeild (Cooper 1969). However, as the wind velocity increases, the convective heat loss from the glass cover to ambient increses. Hence the glass cover temperature increases thereby decreasing the glass cover temperature. This increases the water to glass cover temperature difference and hence the overall yield (Cooper 1969; Dahiru *et al*, 2005).

### **2.6.2 Effect of Ambient Temperature**

Decrease in the ambient temperature decreases the glass temperature and thus the difference ( $T_w - T_g$ ) increases. Numerical results of some researchers e.g. Seithi (2009) and Nafey *et al* (2000) showed that a slight increase of 3% in the solar still productivity is obtained by decreasing the ambient temperature by 5°C.

### **2.6.3 Effect of Solar Radiation and Loss Coefficient**

Solar insolation is an important parameter in the determination of the yield of a solar still. The general output will, to an extent, depend on the distribution of the solar radiation throughout the day. However, this is a second order effect and it is usually sufficient to take into account the total solar radiation recieved on each day. The yeild is maximum when the daily insolation and the mean ambient temperature

are consistently high, with low loss coefficient. The loss coefficient has less influence at higher ambient temperatures (Tiwari 2002).

#### **2.6.4 *Effect of Double-glass Cover and Cover Inclination***

The effect of thermal barrier between the two glass covers impedes the rejection of heat through the condenser, resulting into output reduction. Even with very high water temperatures the governing factor is the low water to glass temperature difference. Although high water temperature leads to high evaporation, the low temperature difference results in a considerable reduction in total energy transfer. The high water temperature causes greater base and side losses. Increasing the value of the thermal conductance of air in between glass, will result in a slightly improved performance, but the combined effect of radiative and convective heat transfer across the air gap in between the glass lowers the output. Also, from the economical and constructional point of view, doubling the glass cover constitutes a substantial part of the total cost of the still which is not desirable.

#### **2.6.5 *Effect of Salt Concentration***

Experiments have indicated that as the salt concentration of the water to be distilled increases right up to the saturation point, the output of the still decreases. However, as the salt concentration of the water increases, there is an increase in the corrosion damage to the components of the still and thus it becomes necessary to use materials which cannot be readily oxidized (Malik *et al* 1982; Adhikari *et al* 1995).

#### **2.6.6 *Effect of Thermal Capacity and Water Depth***

Cooper (1969) as reported in Tiwari, (2002) has studied the effect of water depth on the distillate output as shown in Figure 2.2. The figure reported shows that for an uninsulated still, the gains from decreasing the water depth are only marginal, but with insulation, the difference is more pronounced particularly at lower water depth.

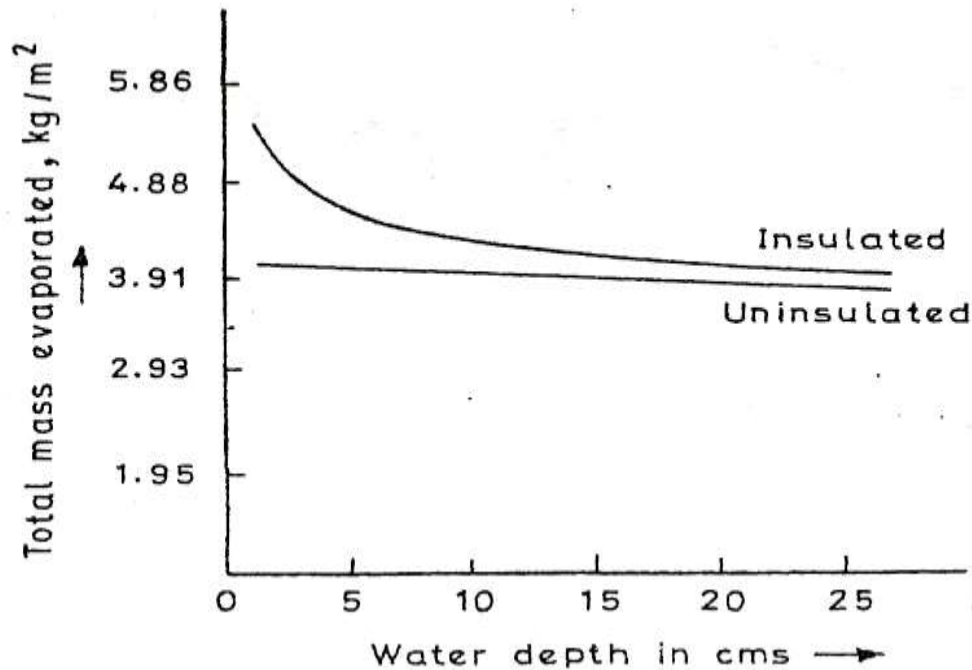


**Figure 2.2: The Effect of Water Depth on Daily Yield (Source: Tiwari 2002).**

**2.6.7 Effect of Charcoal Pieces on the Still Performance**

Charcoal pieces because of their wettability, large absorption coefficient for solar radiation and their ability to scatter rather than to reflect the solar radiation, increases the performance of a solar still. As concluded from the studies done by Mona *et al* (2002), the presence of charcoal pieces utilises the diffuse radiation much better than the conventional unlined still therefore increases yield. The effect is most pronounced in the mornings and on cloudy days when the values of direct radiation are low. The charcoal lined solar still is relatively insensitive to basin-water depth as long as a good amount of the charcoal remains exposed.

**2.6.8 Effect of the Formation of Algae and Mineral Layers on Water and Basin liner**

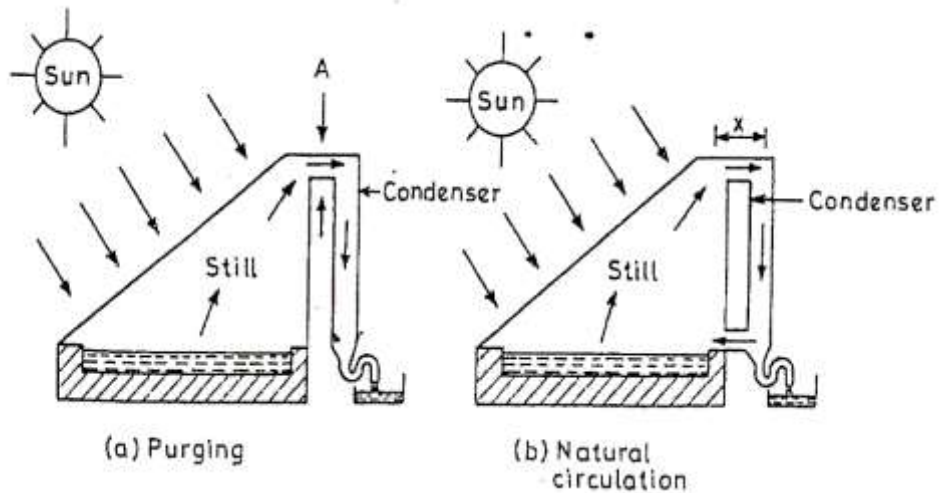
The presence of deposits on the surface of the basin water and basin liner have a detrimental effect on the output, assuming that no other factors become significant. It was shown that the surface reflection appears to be more detrimental than the basin liner reflection because of the absorbing property of the later, except at normal insolation (Cooper 1969).

## **2.7 Various Designs of Solar Still**

Since the daily yield per  $m^2$  per day in a single basin solar still mainly depends on the temperature difference between the evaporative and the condensing surfaces, ( $T_w - T_g$ ), several scientists had made an attempt to maximise the daily yield in a single basin solar still. They employ different designs to get maximum temperature difference between the water surface and the glass cover. Some of the developed designs are as follows:

### **2.7.1 *Single Slope Solar Still with Condenser***

In a conventional solar still, the glass cover is used for transmission of solar energy as well as for condensation of the water vapour evaporated from the water surface. During the condensation, the latent heat is given to the glass cover which raises the glass cover temperature and hence reducing the temperature difference between the evaporative and the condensing surface. In order to increase this difference, the condensing surface is separated from the solar still chamber, as described by Faith (1998) in Tiwari (2002). This can be seen in Figures 2.3 (a) and (b). There is a little condensation on the slope surface, while the main condensation is done by the help of the attached condenser due to transfer (purging) of water vapour from the solar-still chamber to the condensing chamber. Since most of the condensation is taking place in the condensing chamber, the temperature difference between the glasscover and water is more which causes faster evaporation and distillate output is more. In this case, the still efficiency is increased to 45% (Tiwari 2002). Furthermore, the output can be increased by natural circulation as shown in Figure 2.3 (b).



**Figures 2.3(a - b): Single Slope Solar Still with Condenser (Source: Tiwari 2002)**

### 2.7.2 Hybrid Single Slope Still

In this design, the condensing chamber is more improved for faster condensation as shown in Figure 2.4. The proposed change in design uses an electrically operated fan and condensing chamber to increase the distillate output. This is referred to as Hybrid solar distillation system. The active component which is the electrical blower and condenser is attached with the distillation unit.

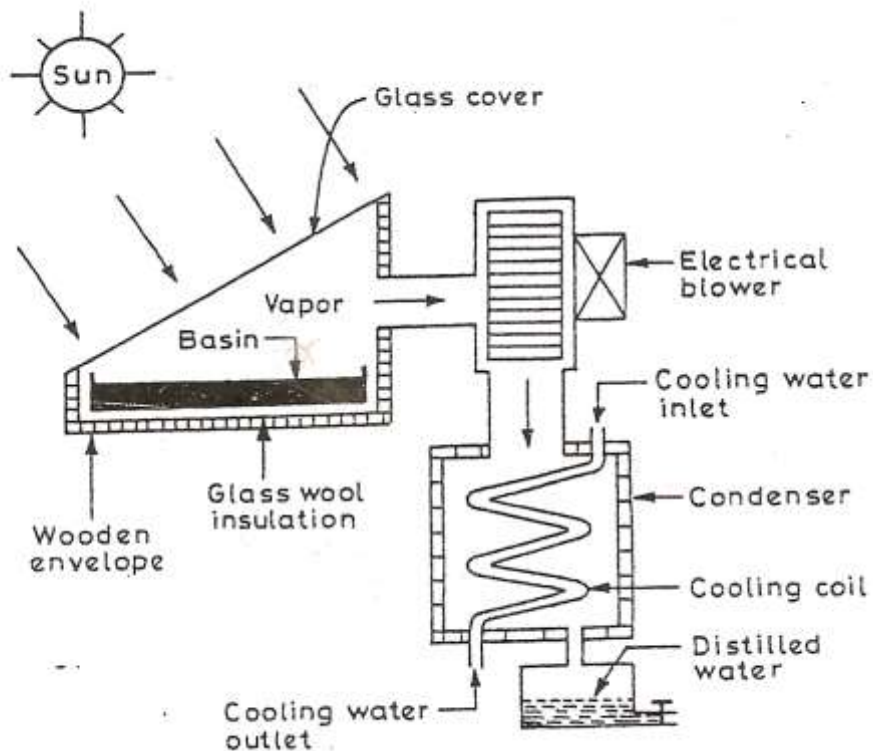


**Figure 2.4: Hybrid Solar Distillation System (Source: Abu-Qudais et al 1996)**

### 2.7.3 Reverse Absorber Solar Still

In this design, the condensing cover is separated from the surface receiving ( $G_1$ ) solar energy as shown in Figure 2.5, unlike the convectional solar still. The solar radiation is allowed to be absorbed at the bottom of the solar still after transmission through the glass cover ( $G_1$ ). This design consists of a cylindrical reflector integrated to the solar still and is based on the concept of an inverted absorber flat plate collector. The solar energy traversing glass cover  $G_1$  is reflected by the mirror through the glass plate  $G_2$  on to the absorber plate (P) which conducts the heat to the water mass by convection. The evaporated water is condensed on inner surface of the condensing cover after releasing its latent heat of condensation. The condensed water trickles down under gravity to the drainage provided at the lower end of the condensing cover. Due to separation of the condensing cover (cold surface) and the surface receiving the solar energy, the temperature difference between the water surface and the condensing cover ( $T_w - T_g$ ) is increased bringing about a higher yield.

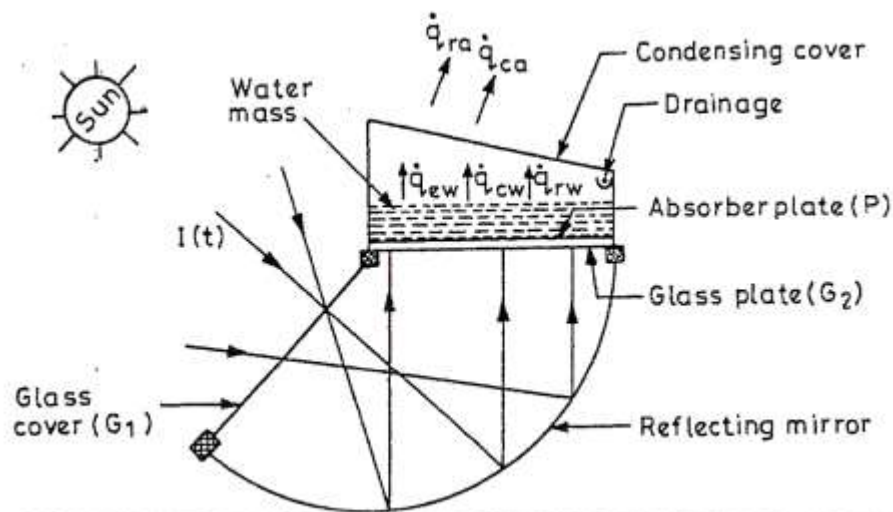


**Figure 2.5:** Schematic View of Reverse Absorber Solar Still (Source: Tiwari and Suneja 1998)

### 2.7.4 Multi-Wick Solar Still

The maximum temperature difference between the condensing cover and the water surface can be achieved by reducing the heat capacity of the water mass in the basin. This was achieved through a design by Sodha *et al* (1981) in Tiwari (2002). A water film is maintained on the absorber for fast heating and quick evaporation. The water film is achieved by using a porous multi-wick (jute cloth) as shown in Figure

2.6. Each jute cloth layer is separated from the other by providing a black polythene sheet so that each can act independently. One end of the jute cloth sheet is dipped in the water reservoir and the other ends are spread over the base of the solar still. Jute cloth soaks the water from the reservoir due to capillary to the inclined surface. The surface is inclined to an optimum angle to receive maximum solar radiation. The glass cover is placed over the unit for condensation of the vapour on its inner surface. The solar radiation is absorbed by blackened jute cloth after transition from the glass cover. The water in the cloth gets heated and evaporation takes place. The evaporated water is condensed on the inner surface of the glass cover after releasing its latent heat of condensation to the glass cover. The released latent heat of condensation is lost to the atmosphere by convection and radiation. The condensed water is trickled down under gravity to the channel provided at the lower end of the solar still. The body of the solarstill is made up of fiber reinforced plastic (FRP) material.

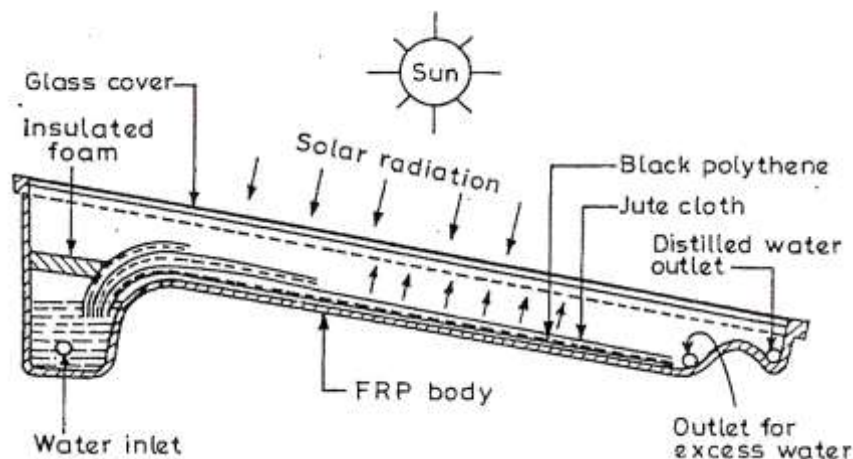


**Figure 2.6: Cross-sectional view of Multi-wick solar still (Source: Sodha et al 1981)**

### 2.7.5 Conical Solar Still

The temperature difference between the evaporating and the condensing surface can also be increased by fast cooling the condensing surface. This is achieved by increasing the heat transfer coefficient from the condensing surface to atmosphere. This can be obtained by increasing the surface area as shown in Figure 2.7, a design by Malik *et al* (1982) in Tiwari (2002). In this design, impure water is enclosed in a transparent twin-arm arrangement. Solar energy trapped within the enclosure heats up the water which causes evaporation and then condensation of the inner surface of the

transparent upper cone. Condensed water droplets slide down in the water pan and are collected in the bottom cone.

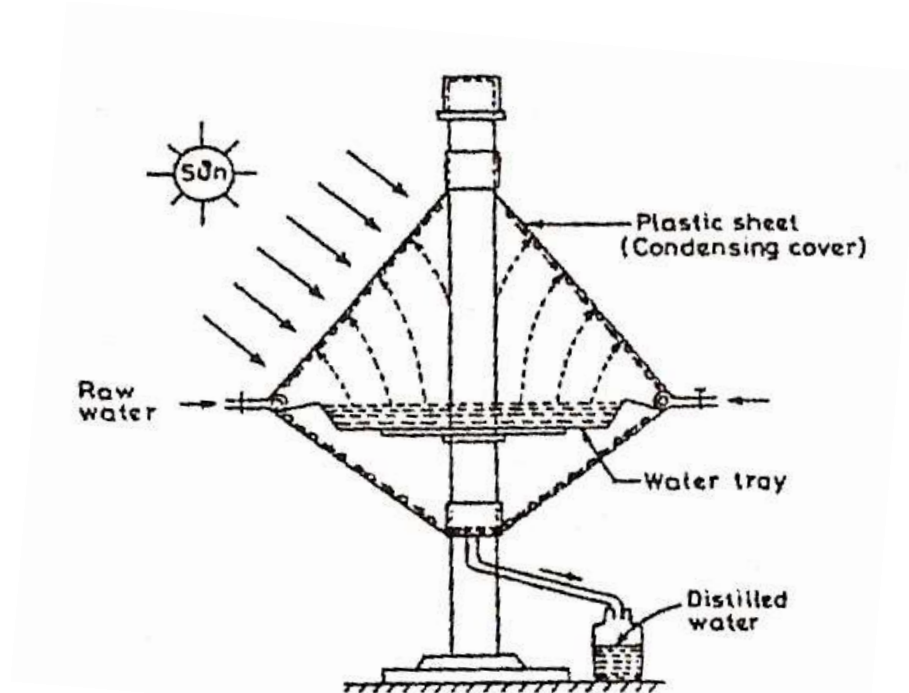


*Figure 2.7: Schematic view of a conical solar still (Source: Malik et al 1982)*

### **2.7.6 Active Single Slope Solar Still**

In the design of the active solar still, the temperature difference between the evaporating and condensing surfaces are increased by feeding the additional thermal energy from the flat plate collector in to the basin of the solar still as shown in Figure 2.8. The flat plate collector is integrated to the basin of the solar still.

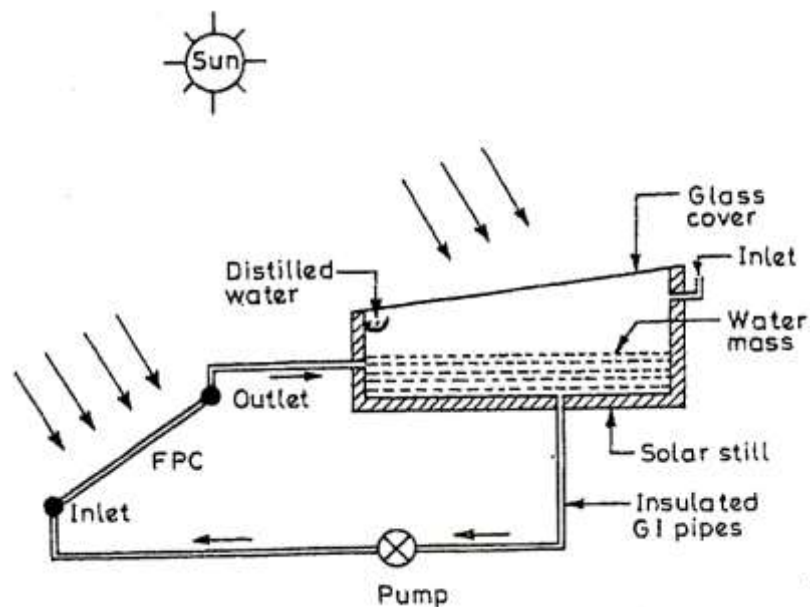


***Figure 2.8: A Schematic view of active solar still with single collector (Source: Kumar and Tiwari 1996)***

The water in the basin is circulated through the flat plate collector either in a natural circulation mode or a forced circulation mode depending on the requirement. The connecting pipes are insulated to avoid thermal losses from the hot water in the pipe to ambient during hot water circulation through it. In an active solar still, the water in the basin is heated directly as well as indirectly through a flat plate collector. The collector should be operated only during the sunshine hour. The rise in the temperature of water in the basin mainly depends on number of collectors connected in series as shown in Figure 2.9.

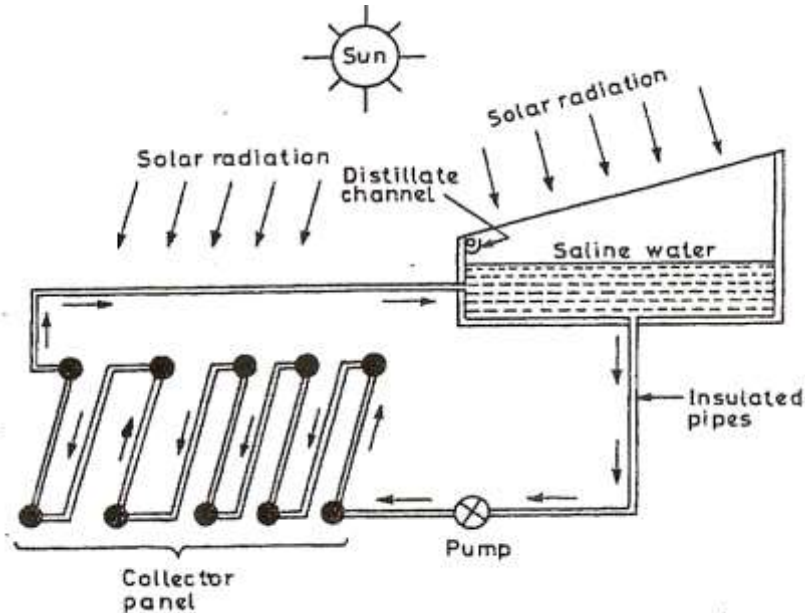


**Figure 2.9:** A Schematic view of active solar still with number of collectors connected in series (Source: Kumar and Tiwari 1996)

In all the foregoing solar still designs, the quality of the distillate produced has to conform with the national and international standards (i.e the World Health Organization, WHO, National Food Drug Administration Agency, NAFDAC) of a standard distilled water: A water that has many of its impurities removed (Howard 2011).

## 2.8 Modelling As a Tool for Physics Research

Models are vehicles for learning about the world. Significant parts of scientific investigation especially Physics researches are carried out on models rather than on reality itself. This is because through models one can discover features of and ascertain facts about the system in which the model stands for (Wimsalt 1987 and Swoyer 1991). In brief, modelling allows for surrogate reasoning. For instance, we study the nature of Hydrogen atom, quantum statistical applications to particles or the behaviour of polymers by studying their respective models. This cognitive function of modelling has been widely acknowledged in Physical researches, which suggest that modelling gives rise to a new style of reasoning, so called model based on reasoning (Magnani *et al* 1999, Magnani and Nancy 2002).

To learn through modelling and or develop models, we begin by establishing a representative relation ('denotation') between the model and the target. Then we investigate the features of the model in order to demonstrate certain theoretical claims about its internal constituents or mechanism ('demonstration'). Finally, these findings have to be converted into claims about the target system ('interpretation') (Hughes 1997).

There are no fixed rules in the construction and the manipulation of models (Morgan 1999) but depending on the kind of model we are trying to develop. In Physics, theoretical modelling amounts to different activities demanding different methodologies.

## **2.9 Review of Some Relevant Researches on Solar Still Modelling**

Solar distillation represents a most attractive and simple technique among other distillation processes and is especially suited to small-scale units at locations where solar radiation is considerable (Mona *et al* 2002). Accordingly, it seems necessary to search for solar stills that are easy to construct and that could provide us with the necessary daily amount of fresh water, not forgetting the drought that has been prevailing in several areas of Africa for the last two decades (Malgwi and Bumba 2003, Ala and Umar 2005).

Numerous attempts have been made by many researchers in order to produce fresh water by means of solar energy. The simple solar still of the static basin type is the oldest method and improvements in its design have been made to increase its efficiency (Al-Hallaj *et al* 1999; Garba *et al* 1996; Bachir 2002, Dahiru *et al* 2005 and Omar 2011).

Howe and Theimat (1974) reviewed twenty years of works on solar distillation carried out at the Sea-water Conversion Laboratory, University of California. One year later, Delyannis and Delyannis (1985) reviewed the major solar distillation plants around the world. In most of these, covers made of glass were used and the black lining was either asphalt or black butyl rubber. They compared the annual operating costs of the different solar stills visited to the cost of water production. The result was that the profit is better for smaller distiller units than the bigger one which they attributed to the cost of the land covered and the man power cost for big solar still plants.

In a study by Mowla and Karimi (1995), a mathematical modelling of solar stills in Shiraz South-Western Iran was proposed and a static basin type consisting of a flat plate collector made of glass was designed. The experimental and theoretical results agree well with little over-estimate on the theoretical result. The average deviation was about 5.1% for the rate of water produced by the model. The discrepancy was as a result of some experimental errors one of which is that probably some distilled water drops back into the basin water. From the results it was found out that the rate of distilled water produced is inversely proportional to the water depth in the basin.

In an article by Bemporad (1995) entitled “Basic hydrodynamic aspects of a solar energy based desalination process”, an investigation was carried out to analyse a theoretical feasibility scheme. The proposed scheme exploits the vapour pressure difference between fluids of different salinities and temperatures to produce fresh water from sea water. He developed a mathematical model to simulate unsteady mass, heat and solute transfer during the desalination process. The governing equations were integrated numerically in space and time through a finite difference technique. The numerical simulations considered both steady-state and time dependent heat sources. The results proved the theoretical feasibility of the proposed desalination scheme. However, the presence of an unsteady heat sources, typical to solar energy based schemes, leads to an unstable density profile in the water column. The unsteady heat flow reduced the efficiency.

In another study carried out by Adhikari *et al* (1995), a computer simulation model for studying the steady-state performance of a multi-stage stacked tray solar still was presented. The model was validated by the results of simulated experiment on a three-stage unit having an immersion type electric heater as the heating source. The results obtained from the models are in good agreement with the experiments. Numerical results are also presented so as to appreciate the relative performance of the proposed multi-stage stacked tray solar still with diffusion type instrumentation.

Garba *et al* (1996), investigated the effect of some meteorological parameters on the performance of a basin-type solar still for distilled water production. The study was carried out in Sokoto, Nigeria and the parameters considered were the ambient temperature, daily solar insolation and wind speed. The results show that there was an increase in the solar stills yield with increase in these parameters. Therefore, these

parameters should be high for an optimum performance. They constructed the still with which they obtained the results using the available materials.

Harpreet (1996) proposed a computer simulation for a solar still with an enlarged evaporation area in order to explore the quantitative relationship between the evaporation area and the distilled water production. The results showed a gain of 19.6% in the yield when the evaporation area was quadrupled, and an asymptotic (infinite area) gain of around 30.2%. A thermodynamic analysis of the two separate energy conversion processes occurring within the still led to “availability” based definition of efficiencies for the collector and the evaporator-condenser. The analysis showed that all of the asymptotic improvement in yield is attributed to the more efficient evaporation-condensation process in the still with enlarged evaporation area. The analysis also suggested that stills with enlarged evaporation area could be operated on cheap low temperature thermal energy such as that from solar ponds.

A solar still in which charcoal functions both as heat absorber medium and as wick has been constructed by Mona and Marvat (2002). The still presents a 15% improvement in productivity over wick-type stills. The still is non-conventional, cheap, simple, easy to construct and operate and is of low thermal capacity. The results show that coarse charcoal granules give acceptable results at high flow rates followed by intermediate then fine granules. The still was postulated to be used in waste water treatment coupled with production of portable water. Also variable bed thickness can be used for efficient removal of pollutants from the waste-water.

Bachir (2002), worked on solar desalination plant for domestic needs in arid areas of south Algeria. The performance of a solar still where the fed water is brackish underground geothermal water was determined under the actual insulation at the south Algeria. Theoretical analyses of the heat and mass transfer mechanisms inside the still have been developed. The measured performance was then compared with the results obtained by theoretical analyses. The results show that the efficiency increases with the increase in solar radiation flux and with the increase in brine temperature. Also, the efficiency increases when there is a recovery of latent heat of condensation.

Dahiru *et al* (2005), worked on the performance evaluation of a basin-type solar still in Yola (9.23°N, 23°E). They constructed a basin-type solar still using the locally available materials which cut down the construction cost, hence producing the distillate at a cheaper rate. The still’s operating efficiency according to them was (25-

46)%. The performance test was conducted in the months of September, a period characterised with heavy rainfall and cloud cover in the study area. A total distillate of 329 ml was collected daily over a time ranging from 7.00 a.m. to 4.00 p.m (Local Time).

A study on the impact of temperature difference (water-collector) on solar still global efficiency was conducted by Kaabi and Smakdji (2007). They developed a mathematical model aided by some basic and simplified hypothesis, according to overall thermal balances and appropriate heat and mass coefficients. They resolved the equations based on finite difference method. The results show that a better efficiency is obtained at a maximum temperature difference, low glass thickness, a gradient (angle of inclination) closer to that of the area latitude in which the solar still was placed and high wind velocity. The results of the study elaborate the importance of cooled condensation and hotter evaporation surfaces.

## **2.10 Present Works on Solar Stills**

The implementation programme of solar stills is presently at its beginning stage (Garba *et al* 1996). Delhi Energy Development Agency has installed 200 stills each of area 1.0 m<sup>2</sup> with a nominal capacity of 3 to 4 litres per day each. The stills are of single basin type with glass cover (Garba *et al* 1996).

Scientists e.g Kaabi and Smakdji 2007, Harpreet 1996, Mona and Marvat 2002 and Bachir 2002, developed theoretical models in Constantine, Algeria, Madras-India and South Algeria respectively for different designs of solar still.

Here in Nigeria, the Sokoto Energy Research Centre has developed different designs and mathematical models of solar stills with an average yield of less than 3.3 litres per m<sup>2</sup> of still area per day. Plots of various metrological parameters with time were obtained. The correlation result indicated that the solar radiation and the ambient air temperature have good correlations whereas other parameters like relative humidity have very poor correlation with the yield (Sambo and Aliyu 1992).

Also, the research done in Yola by Dahiru *et al*, (2005) determine the results of variation of some meterological data with time and or distillate in the month of September only with total daily out-put of 329 ml as reported earlier. This could not be a good approximation for the fact that the work was done during the time of the

year when cloud cover is likely to be heavy. More so, the time span was from 7 a.m. to 4 p.m, (Local Time) does not cover sun shine hours of the day.

In view of the above predicaments this work develops a theoretical model of solar still in Yola, ( $9.23^{\circ}\text{N}$ ,  $13^{\circ}\text{E}$ ). A static flat plate basin-type solar still was constructed and measurements taken over period extending beyond 4 pm local time during dry and wet seasons. In the construction, most of the problems stated were taken into consideration.

## CHAPTER THREE

### MATERIALS AND METHODS

#### 3.1 Introduction

The methods adopted in this research comprised of developing a theoretical model for a single glass plate, passive solar still performance and then construct a simple still to test the model. This chapter therefore, has contents of the theoretical formulations for the solar still after surveying the study area. The formulation takes care of the design correction factor e.g. ratio of the slope area to the basin area. The result obtained from the model equation shall afterward be compared with that of a constructed distiller unit. The detailed design of the experimental distiller used in taking experimental data which was done for comparison with that obtained from the theoretical model equation is also discussed.

#### 3.2 Theory of Solar Still

A solar still is device used for converting brackish water into portable water using solar energy. A solar still essentially consists of a mass of water in a container, which is covered by a transparent cover and the interior surface of this enclosure is coated black to absorb solar radiation entering through the condensation of water vapour. The cover is sloped on one side to enable the condensate to trickle into a trough. The whole enclosure is insulated to minimize heat losses from the sides and the bottom surface. (See fig. 3.1).

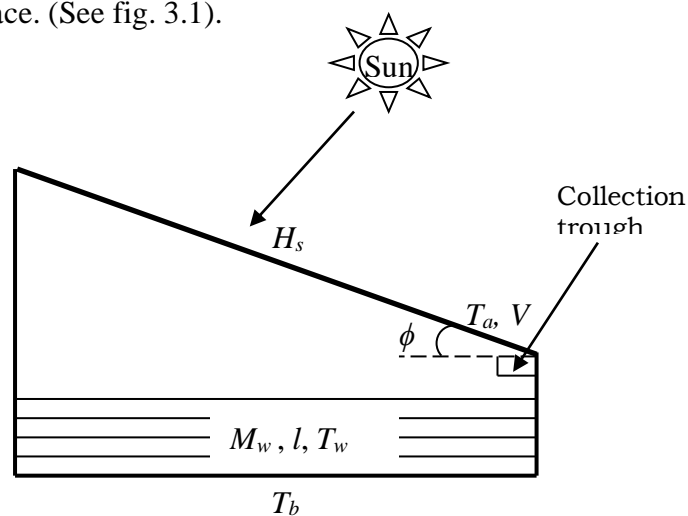


*Figure 3.1: A typical Single slope conventional solar still. See Appendix A for definitions of the parameters  $M_w, l, T_w, T_a, T_b, H_s$  and  $V$ .*

The glass cover permits solar radiation to get into the still, which is absorbed predominantly by the black base. Consequently, the water gets heated up and hence the moisture content of the air trapped between the water surface and the glass cover increases. The base also radiates energy in the infrared region which is mainly absorbed by water in the basin. Thus, the glass cover traps the solar energy inside the still; it also reduces the convective heat losses. The glass cover is usually sloped to enable the water vapour which condenses on the interior surface to trickle in to a slightly slanted collecting trough which was finally collected through the out let.

Different aspects of solar stills have been theoretically examined by different researchers thereby developing different models with the aim of improving the thermal efficiency and the yield (Tleimat and Howe 1966, Malik and Van Tran 1973, El-Nashar 1992, Ghandhidasan and Abdulhamayel 1994, Porta *et al* 1997, Nafey *et al*, 2000 and Tiwari 2002).

A common approach to modelling solar stills is the use of energy balance equations in which the input solar energy is balanced against the useful output energy and various losses from the system. It should be noted that the law of conservation of energy is vital in the analysis of heat transfer to and from a system. Tiwari (2002) reported that correlations for the internal heat and mass transfer in a conventional solar developed by Dunkle (1961) are used in most studies on solar still modelling.

### 3.3 Thermal Analysis and the Energy Balance

#### 3.3.1 The Energy Balances

The basin heat flux components at various points are as shown in Figure (3.2)

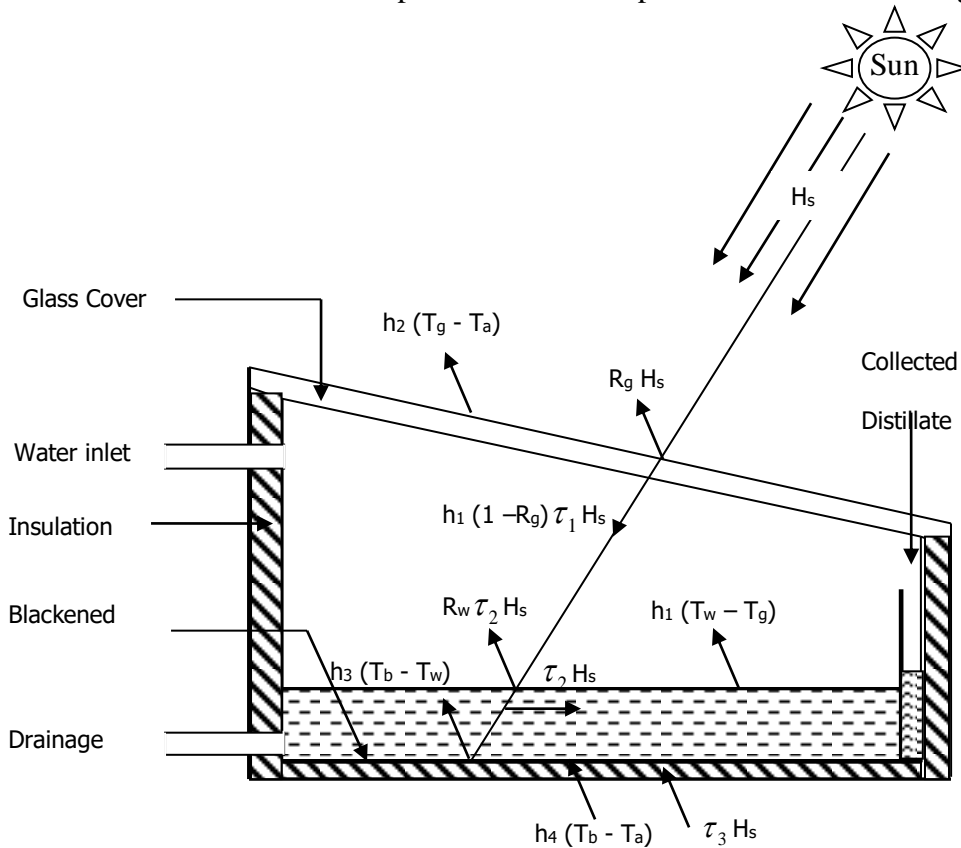


**Figure 3.2: A typical Single slope basin solar still: Schematic diagram Showing energy balances. All parameters are defined in Appendix A.**

The energy balance for the different components of the still is as follows:

#### (i) Glass cover

The energy balance for the glass cover can be expressed as

$$\tau_1 H_s + [\dot{q}_{rw} + \dot{q}_{cw} + \dot{q}_{ew}] = \dot{q}_{rg} + \dot{q}_{cg} \quad (3.1)$$

Rate of energy absorbed	Rate of energy received from water surface by (i) Radiation (ii) Convection (iii) Evaporation	Rate of energy lost to air
-------------------------	--	----------------------------

where  $\tau_1$  is the solar flux absorbed by the glass cover,  $H_s$  is the solar insolation,  $\dot{q}_{rw}$  is the radiative heat loss to water,  $\dot{q}_{cw}$  is the convective heat loss to water,  $\dot{q}_{ew}$  is the

evaporative heat loss from the water,  $\dot{q}_{rg}$  is the radiative heat loss to glass and  $\dot{q}_{cg}$  is the convective heat loss to glass.

**(ii) The water content (water mass)**

The balance for the water content inside the solar still is

$$\tau_2 H_s + \dot{q}_w = M_w C_w \frac{dT_w}{dt} + \dot{q}_{rw} + \dot{q}_{cw} + \dot{q}_{ew} \quad (3.2)$$

Rate of energy absorbed	Rate of energy convected from the basin liner	Rate of energy stored	Rate of energy transferred to glass cover from water by (i) Radiation (ii) Convection (iii) Evaporation
-------------------------	---	-----------------------	--

where  $\tau_2$  is the solar flux absorbed by the water mass,  $M_w$  is the mass of the water inside the basin  $C_w$  is the specific heat capacity of the water  $T_w$  is the water temperature and  $t$  is the period of measurement.

**(iii) The basin liner**

The energy balance for the basin liner of the still is expressed as

$$\tau_3 H_s = \dot{q}_w + \left[ \dot{q}_b + \dot{q}_b \left( \frac{A_s}{A_b} \right) \right] \quad (3.3)$$

Rate of energy absorbed	Rate of energy transferred to water	Rate of energy lost through the bottom and side walls by conduction
-------------------------	-------------------------------------	---

where  $\tau_3$  is the solar flux absorbed by the basin,  $\dot{q}_w$  is the rate of heat transferred to water,  $\dot{q}_b$  is the rate of heat transferred to the basin,  $A_s$  is the total still area and  $A_b$  is the still bottom area.

The heat transfer coefficient,  $\dot{q}$  appearing in equations (3.1) to (3.3) are the external and internal heat transfer coefficients as explained below

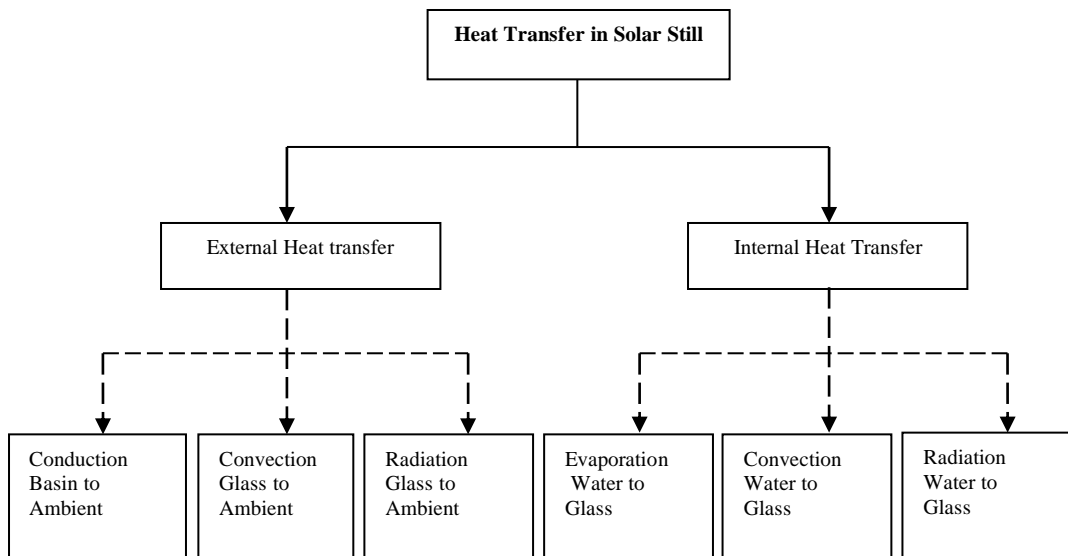
### 3.4 The Heat Transfers

In solar distillation systems, heat transfer can be classified into two categories, the internal and external modes of heat transfers (Tiwari 2002; Aminul and Teruyuki 2010).

The external heat transfer occurs outside the distiller unit, from the glass cover, side wall and the bottom insulation. It is the mode of heat transfer in which the conduction, convection and radiation processes are independent of each other.

The internal heat transfer on the other hand is the heat transfer within the distiller unit. This consists of the radiative, convective and evaporative heat transfers. In this case, the convective heat transfer occurs simultaneously with the evaporative heat transfer and these two are independent of radiative heat transfer.

**Table: 3.1: Heat and Mass Transfer Classification in Conventional Solar Still (Source: Tiwari, 2002)**



### 3.5 The External Heat Transfer

The external heat transfer in solar still is mainly through conduction, convection and radiation processes which are independent of each other. Therefore, here we are going to treat each independently in the following sub sections.

### 3.5.1 Top Loss Coefficient

The glass thickness in most cases is very small. Therefore the temperature in the glass is assumed uniform. The external heat transfer loss by radiation and convection from the glass cover to ambient,  $\dot{q}_g$  can be expressed as

$$\dot{q}_g = \dot{q}_{rg} + \dot{q}_{cg} \quad (3.4)$$

The radiative heat transfer from the glass cover to ambient is given in (Tiwari, 2002) as

$$\dot{q}_{rg} = h_{rg} (T_g - T_a) \quad (3.5)$$

where  $T_g$  and  $T_a$  are the glass and ambient Temperatures,  $h_{rg}$  is the radiative heat transfer coefficient from the glass cover to ambient given as

$$h_{rg} = \varepsilon_g \sigma \left[ \frac{(T_g + 273)^4 - (T_{sky} + 273)^4}{(T_g - T_a)} \right] \quad (3.6)$$

where  $\varepsilon_g$  is the emissivity of the glass,  $\sigma$  is the Stefan's constant and  $T_{sky}$  is the sky temperature being related to ambient as

$$T_{sky} = T_a - 6 \quad (3.7)$$

The convective heat transfer from glass cover to the ambient is also given as

$$\dot{q}_{cg} = h_{cg} (T_g - T_a) \quad (3.8)$$

where  $h_{cg}$  is the convective heat transfer coefficient from the glass cover to ambient.

Substituting (3.5) and (3.8) in (3.4) we get

$$\dot{q}_g = h_1 (T_g - T_a) \quad (3.9)$$

where  $h_1$  is the total external heat transfer coefficient written as

$$h_1 = h_{rg} + h_{cg} \quad (3.10)$$

It should be noted that in setting the energy balance equations (3.1 to 3.3) the side area  $A_{sw}$  being very small in comparison to the basin liner area,  $A_b$  of the solar still, the term  $A_{sw}/A_b$  can be neglected. On substituting the values for the heat transfer losses,  $\dot{q}$  Equations (3.1) to (3.3) can be rewritten as

$$\tau_1 H_s + h_{1w}(T_w - T_g) = h_{1g}(T_g - T_a) \quad (3.11)$$

$$\tau_2 H_s + h_1(T_b - T_w) = M_w c_w \frac{dT_w}{dt} + h_2(T_w - T_g) \quad (3.12)$$

$$\tau_3 H_s = h_1(T_b - T_w) + h_3(T_b - T_a) \quad (3.13)$$

Substituting the values of  $T_g$  and  $T_b$  from (3.11) and (3.13) into (3.12) and simplify, we get

$$\frac{dT_w}{dt} + aT_w = f(t) \quad (3.14)$$

where

$$a = \frac{U_L}{M_w c_w} \quad (3.15)$$

$$f(t) = \frac{(\alpha\tau)_{eff} H_s + U_L T_a}{M_w c_w} \quad (3.16)$$

$$(\alpha\tau)_{eff} = \tau_3 \frac{h_1}{h_3 + h_4} + \tau_2 + \tau_1 \frac{h_2}{h_1 + h_2} \quad (3.17)$$

$$U_L = U_t + U_b \quad (3.18)$$

$$U_L = U_t + U_b = \frac{h_3 h_4}{h_3 + h_4} + \frac{h_1 h_2}{h_1 + h_2} \quad (3.19)$$

To obtain an approximate numerical solution of equation (3.14) it was assume that: the time interval  $\Delta t$  is small; the function  $f(t)$  is constant that is  $f(t) = \overline{f(t)}$  for the time interval  $\Delta t$  and  $a$  is also constant during the time interval  $\Delta t$ . The value of  $h_1$  can be determined after considering the known values of  $T_w$  and  $T_g$  at  $t = 0$ , that is

$$T_w|_{t=0} = T_{w0} \quad \text{and} \quad T_g|_{t=0} = T_{g0} \quad (3.20)$$

Then solution to equation (3.14) can be derived as follows

$$T_w = \frac{\overline{f(t)}}{a} (1 - e^{-a\Delta t}) + T_{w0} e^{-a\Delta t} \quad (3.21)$$

where  $T_{w0}$  is the temperature of the basin water at  $t = 0$  and  $\overline{f(t)}$  is the average value of  $f(t)$  for the time interval  $\Delta t$ .

The average temperature of water  $T_w$  is given by

$$\overline{T_w} = \frac{1}{t} \int_0^t T_w dt \quad (3.22)$$

or

$$\overline{T_w} = \frac{\overline{f(t)}}{a} \left[ 1 - \frac{(1 - e^{-a\Delta t})}{a\Delta t} \right] + T_{w0} \frac{(1 - e^{-a\Delta t})}{a\Delta t} \quad (3.23)$$

The average glass temperature in terms of the water temperature can be obtained from equation (3.11) as

$$\overline{T_g} = \frac{\tau_1 H_s(t) + h_1 \overline{T_w} + h_1 \overline{T_a}}{h_1 + h_2} \quad (3.24)$$

From equation (3.23),  $T_w$  can be calculated as a function of time. At any time the heat flux due to the evaporation can be written as:

$$Q_{ew} = h_{ew} (T_w - T_g) \quad (3.25)$$

or

$$Q_{ew} = \frac{h_{ew} h_2}{h_2 + h_1} (T_w - T_a) \quad (3.26)$$

and the hourly yield of evaporated water is given by

$$m = \frac{Q_{ew}}{\lambda} = \frac{h_{ew} (T_w - T_g)}{\lambda} \times 360 \text{ kg/m}^2\text{h} \quad (3.27)$$

After obtaining the timely yield, the value of  $M_w C_w$  for the next interval reduces by  $mC$  as such for the next interval it becomes  $M_w C_w - m c_w$

The instantaneous efficiency,  $\eta_i$  of a solar still, is ratio of the energy used for water production to the total radiation rate is given by:

$$\eta_i = \frac{Q_{ew} A_b}{H_s A_b} = \frac{Q_{ew}}{H_s} = \frac{h_{ew} (T_w - T_g)}{H_s} \quad (3.28)$$

and from equation (3.26) we can write

$$\eta_i = \frac{h_{ew}h_2}{h_1 + h_2} (T_w - T_a) \quad (3.29)$$

The above equation can be rewritten by substituting the value of  $T_w$  from equation (3.23) as

$$\eta = \frac{h_{ew}h_2}{h_1 + h_2} \frac{1}{U_L} \times \left[ (\alpha\tau)_{eff} (1 - e^{-a\Delta t}) + U_L \frac{(T_{w0} - T_a)}{H_s} e^{-a\Delta t} \right] \quad (3.30)$$

It should be noted that (3.30) does not include the side wall and top cover correction factors. It is in view of this that the present model was design to take care of these correction factors.

### 3.6 The Theoretical Modelling

In this modelling, a conventional solar still made of galvanized iron sheet in a square base rectangular shape was also considered. The top cover is made of glass sloped at an angle equal to the latitude of the point of research (MAUTECH Yola) and the interior surface is painted black for the maximum absorption of solar energy. Saline water was poured into the still to fill it partially and then exposed to the Sun.

The following assumptions have been made in writing the energy balance in terms of Joule per second per m<sup>2</sup>:

- (i) Inclination of the glass cover is the same as the latitude of the place of research, Modibbo Adama University of Technology, Yola (= 9.23°)
- (ii) The heat capacity of the glass cover, the absorbing material and the insulation (bottom and sides) are neglected
- (iii) There is no leakage in the solar distiller.

Normally, the total external heat transfer coefficients,  $h_l$  from equation (3.10) is expressed empirically for two cases based on how the effects of free convection and radiation from the glass are treated as follows

**Case (i):** In this case, the expression includes the effect of free convection and radiation from the glass cover as discussed by McAdams (1954) (Mowla and Karimi 1995; Ilaria *et al* 2010). The expression is

$$h_1 = 5.7 + 3.8 V \quad \text{for } 0 \leq V \leq 5 \text{ms}^{-1} \quad (3.31)$$

where  $V$  is the wind speed measured in m/s. Equation (3.11) for a zero wind speed gives heat loss by natural convection. The process taking place here is not as simple as it appears since the wind may not always be blowing parallel to the surface.

**Case (ii):** Here the radiation and convection losses are to be evaluated separately. The radiative heat transfer coefficient,  $h_{rg}$  can be obtained from equation (3.6) and the convective heat transfer coefficient,  $h_{cg}$ , be obtained from the relation below

$$h_{cg} = 2.8 + 3.0 V \quad \text{for } 0 \leq V \leq 7 \text{ms}^{-1} \quad (3.32)$$

It is clearly stated (Wattmuff *et al*, 1977) that equation (3.32) included the effect of free convection and radiation. More so the numerical solution in either case shows that there is no significant change in the performance of the still (Mowla and Karimi 1995). In this research therefore, we shall adopt equation (3.31) for its straight forwardness.

The total internal heat loss coefficient,  $h_{iw}$  and conductive heat transfer coefficient of the glass,  $(K_g/L_g)$  are expressed in the water heat transfer coefficient as

$$U_{w0} = \left[ (1/h_2) + (L_g / K_g) \right] \quad (3.33)$$

$$U_{w0} = \frac{h_2 (K_g / L_g)}{h_2 + (K_g / L_g)} \quad (3.34)$$

where  $U_{w0}$  is heat transfer coefficient from the water to outside,  $h_2$  is the total internal heat transfer coefficient,  $K_g$  and  $L_g$  are the respective conductivity and thickness of the glass cover.

The overall top loss coefficient,  $U_t$  from the water mass to the ambient through the glass cover was written to include the effect of the top cover correction factor in this model as

$$U_t = \left[ \frac{h_1 h_2}{h_1 + U_{w0}} \right] F_1 \quad (3.35)$$

where  $F_1 = (A_g/A_b)$  is the glass cover correction factor

### 3.6.1 Bottom and Side Loss Coefficient

The rate of heat loss from the basin liner to the ambient per m<sup>2</sup> can be written as

$$\dot{q}_b = h_4(T_b - T_a) \quad (3.36)$$

where

$$h_4 = \left[ \frac{L_i}{K_i} + \frac{1}{h_{cb} + h_{rb}} \right]^{-1} \quad (3.37)$$

The heat lost from the water in the solar still to the ambient through the thick insulation (of thickness,  $L_i$  and conductivity,  $K_i$ ) and subsequently by convection and radiation from the bottom,  $U_b$ , and side surfaces of the basin,  $U_{sw}$ , can be written respectively as

$$U_b = \left[ \frac{1}{h_3} + \frac{1}{h_4} \right]^{-1} = \left[ \frac{1}{h_3} + \frac{1}{K_i/L_i} + \frac{1}{h_{cb} + h_{rb}} \right]^{-1} \quad (3.38)$$

Equation (3.18) can simply be written as

$$U_b = \left[ \frac{h_3 h_4}{h_3 + h_4} \right] \quad (3.39)$$

and

$$U_{sw} = U_b \left( \frac{A_{sw}}{A_b} \right) = \left[ \frac{1}{h_3} + \frac{1}{K_i/L_i} + \frac{1}{h_{cb} + h_{rb}} \right]^{-1} \left( \frac{A_{sw}}{A_b} \right) \quad (3.40)$$

or

$$U_{sw} = \left[ \frac{h_3 h_4}{h_3 + h_4} \right] \left( \frac{A_{sw}}{A_b} \right) \quad (3.41a)$$

Normally, the side wall area,  $A_{sw}$  in contact with the water is very small as compared with the area of base,  $A_b$ . It is in most case neglected as stated earlier (Tiwari 2002; Hiroshi 2010). But in this research it is not. It is included as the correction factor,  $F_2$ . Therefore (3.21) can be rewritten as

$$U_{sw} = \left[ \frac{h_3 h_4}{h_3 + h_4} \right] F_2 \quad (3.41b)$$

where  $F_2 = (A_{sw}/A_b)$  is the side wall correction factor

The overall heat transfer coefficient,  $U_L$  from the water mass to the ambient through the top bottom and sides of the distiller unit is expressed as

$$U_L = U_t + U_b + U_{sw} \quad (3.42)$$

$$U_L = \left[ \frac{h_1 h_2}{h_1 + U_{w0}} \right] F_1 + \left[ \frac{h_3 h_4}{h_3 + h_4} \right] + \left[ \frac{h_3 h_4}{h_3 + h_4} \right] F_2 \quad (3.43)$$

### 3.7 The Internal Heat Transfer

The heat transfer that takes place within the solar still is generally through evaporation, convection and radiation. The convective and evaporative heat transfers occur simultaneously and are independent of the radiative heat transfer.

#### 3.7.1 Radiative Loss Coefficient

Most researchers (Tiwari, 2002; Tsilingiris, 2009; Sethi, 2009 and Tsilingiris, 2010) consider the water surface and the glass cover as parallel, due to the fact that the inclination of the glass cover is very small and that the solar distiller has a large width. But in this research we correct this difference and thus, used the correction factor,  $F_1$  in the development of the model. The rate of radiative heat transfer,  $\dot{q}_{rw}$  from the water surface to the glass for infinite parallel plane is given as

$$\dot{q}_{rw} = h_{rw} (T_w - T_g) \quad (3.44)$$

Again the radiative heat transfer is given in terms of the effective emissivity and Stefan's constant as in Tiwari (2002) and Garba *et al*, (1996) thus

$$\dot{q}_{rw} = \varepsilon_{eff} \sigma \left[ (T_w + 273)^4 - (T_g + 273)^4 \right] \quad (3.45)$$

From equations (3.44) and (3.45) the radiative heat transfer coefficient from the water to the glass cover,  $h_w$  can be obtained as

$$h_{rw} = \varepsilon_{eff} \sigma \left[ \frac{(T_w + 273)^2 + (T_g + 273)^2}{T_w + T_g + 546} \right] \quad (3.46)$$

or

$$h_{rw} = \sigma \left[ \frac{(T_w + 273)^2 + (T_g + 273)^2}{\left( \frac{1}{\varepsilon_w} + \frac{1}{\varepsilon_g} - 1 \right) (T_w + T_g + 546)} \right] \quad (3.47)$$

where

$$\varepsilon_{eff} = \left( \frac{1}{\varepsilon_w} + \frac{1}{\varepsilon_g} - 1 \right)^{-1} \quad (3.48)$$

### 3.7.2 Convective Loss Coefficient

There is a heat transfer across the humid air inside the distiller unit by free convection. This is caused by the effect of buoyancy, due to density variation in the humid fluid, which occurs due to the temperature gradient in this fluid. The rate of heat transfer from the water surface to the glass cover,  $\dot{q}_{cw}$  by convection in the upward direction through the humid fluid can be estimated as

$$\dot{q}_{cw} = h_{cw} (T_w - T_g) \quad (3.49)$$

The internal convective heat transfer coefficient,  $h_{cw}$  from heat flow from the horizontal basin (hottest region in the still) to water mass in the basin and vice-versa is determined from the following relations (Sodah *et al* 1980, Malik *et al* 1982, Egarievwe 1989, Tiwari 2002 and Saini and Saini 2008):

$$Nu = C(Gr \cdot Pr)^n \quad (3.50)$$

where

$$Nu = \frac{h_{cw} X_l}{k_w} \quad (3.51)$$

or

$$h_{cw} = \frac{k_w}{X_l} C (Gr \cdot Pr)^n \quad (3.52)$$

$$Gr = \frac{X_l^3 \rho_w^2 g \beta \Delta T'}{\mu_w^2} \quad (3.53)$$

$$Pr = \frac{C_{pw} \mu_w}{k_w} \quad (3.54)$$

$$\Delta T' = \left[ \Delta T + \frac{(P_w - P_{gi})(T_w + 273)}{2.689 \times 10^5 - P_w} \right] \quad (3.55)$$

$$\Delta T = T_w - T_{gi} \quad (3.56)$$

Normally, the unknown constants  $C$  and  $n$  are calculated by linear regression analysis using experimental data. Equation (3.30) is only valid for a normal operating temperature  $\sim 50$  °C and  $\Delta T' = 17$  °C. The expression for  $Gr$  reduces to (Tiwari, 2002)

$$Gr = 2.81 \times 10 X_l^3 \quad (3.57)$$

**Table 3.2: Value of Grashof number ( $Gr$ ) for different average spacing ( $X_l$ ) (Source Tiwari 2002)**

$X_l$ (m)	$Gr$	$C$	$n$
<b>0.15</b>	$0.948 \times 10^5$	0.21	$\frac{1}{4}$
<b>0.20</b>	$2.248 \times 10^5$	0.21	$\frac{1}{4}$
<b>0.25</b>	$4.390 \times 10^5$	0.075	$\frac{1}{3}$

As can be seen from equation (3.57), the Grashof number depends on the average spacing between the water and the glass cover for a normal operating temperature range (Table 3.3). The table gives the value of  $Gr$  for different  $X_l$ .

Using the constructed distiller, equation (3.57) was used to determine the grashof number. The result obtained was  $Gr = 3.5 \times 10^6$  indicating that its value was within the range  $3.2 \times 10^5 < Gr < 1.00 \times 10^7$ . Therefore, the values of  $C$  and  $n$  appearing in equation (3.50) were chosen based on table (3.4) to be 0.075 and 0.33 respectively.

**Table 3.3: Value of  $C$  and  $n$  for different Grashof number ranges**  
(Source: Tiwari, 2002)

Case	$Gr$	$C$	$n$
<b>I</b>	$Gr < 1.00 \times 10^3$	1.00000	0
	$1.0 \times 10^4 < Gr < 3.25 \times 10^5$	0.21000	$\frac{1}{4}$
	$3.2 \times 10^5 < Gr < 1.00 \times 10^7$	0.07500	$\frac{1}{3}$
	$2.5 \times 10^3 < Gr < 6.00 \times 10^4$	0.07477	0.36
<b>II</b>	$2.5 \times 10^5 < Gr < 1.00 \times 10^7$	0.05238	0.36
	$2.0 \times 10^3 < Gr < 5.00 \times 10^4$	0.05814	0.4
<b>III</b>	$5.0 \times 10^4 < Gr < 2.00 \times 10^5$	3.80000	0.00
	$2.0 \times 10^5 < Gr$	0.04836	0.37
<b>IV</b>	$2.8 \times 10^3 < Gr < 2.10 \times 10^5$	0.30000	$\frac{1}{4}$
	$2.0 \times 10^3 < Gr < 5.00 \times 10^4$	0.12550	$\frac{1}{3}$

After substituting the values of  $Nu$ ,  $Gr$  and  $Pr$  in equation (3.50) the convective heat transfer coefficient  $h_{cw}$  becomes

$$h_{cw} = \frac{C k_w}{X_1} \left[ \frac{X_1^3 \rho_w g \beta \Delta T'}{\mu_w^2} \cdot \frac{C_{pw} \mu_w}{k_w} \right]^{\frac{1}{3}} \quad (3.58)$$

Dunkle (1961) also derived the following expression for  $h_3$  as thus:

$$h_{cw} = 0.884 \left[ (T_w - T_{gi}) + \frac{(P_w - P_g)(T_w + 273)}{2.689 \times 10^5 - P_w} \right]^{\frac{1}{3}} \quad (3.59)$$

The convective heat transfer between the basin and the water is given as

$$\dot{q}_w = h_3(T_b - T_w) \quad (3.60)$$

where the convective heat transfer coefficient,  $h_w$  is given as

$$h_3 = \frac{k_w}{X_w} C(Gr \cdot Pr)^n \quad \text{where } C = 0.54 \text{ and } n = 0.25 \quad (3.61)$$

### 3.7.3 Evaporative Loss Coefficient

The mass transfer coefficient,  $h_e$  in terms of convective heat transfer coefficient,  $h_{cw}$ , the total gas pressure,  $P_T$ , the mass of the water vapour,  $M_w$ , the air mass,  $M_a$ , the specific latent heat,  $L$  and the specific heat per unit volume at constant pressure,  $C_{pa}$  of the mixture is given by Baum (1964) as reported in (Mowla and Karimi 1995; Garba<sup>a</sup> *et al*, 1996; Aminul and Teruyuki 2010) as

$$\frac{h_e}{h_{cw}} = \frac{L}{C_{pa}} \left( \frac{M_w}{M_a} \right) \left( \frac{1}{P_T} \right) \quad (3.62)$$

The expression above is formulated owing to the following assumptions

- (i) the exchange of the water vapour with the boundary layers at both the water and glass surfaces is neglected
- (ii)  $P_w$  and  $P_g$  are considered smaller than  $P_T$

The general equation for the rate of evaporation transfer from the water mass surface in the basin to the glass cover is

$$\dot{q}_{ew} = h_{ew}(T_w - T_g) \quad (3.63)$$

Malik *et al*, (1982) developed a mathematical correlation based on the lewis relation, equation (3.42) for the rate of heat transfer per unit area from the water surface to the glass cover and after substituting the appropriate values for the parameters in equation (3.42) obtained

$$\dot{q}_{ew} = 0.013h_{cw}(P_w - P_g) \quad (3.64)$$

From equations (3.63) and (3.64) we can write  $h_{ew}$  as

$$h_{ew} = 1.6273 \times 10^{-2} h_{cw} \frac{P_w - P_g}{T_w - T_g} \quad (3.65)$$

It is important to mention here that the value of  $h_{ew}$  can be more realistic for larger value of  $(T_w - T_g)$ . The values of  $P_w$  and  $P_g$  (for the range of temperature  $10^\circ\text{C} - 90^\circ\text{C}$ ) can be obtained from the expression (Fernandez and Chargoy 1990).

$$P(T_x) = \exp \left[ 25.317 - \frac{5144}{(T + 273)} \right] \quad (3.66)$$

where  $x$  could be water or glass as the case may be.

The total internal heat transfer coefficient,  $h_2$  is the sum of the three internal heat transfer coefficients viz: the radiative, convective and evaporative heat transfers i.e. equations (3.47), (3.59) and (3.65) thus

$$h_2 = h_{rw} + h_{cw} + h_{ew} \quad (3.67)$$

$$h_2 = \sigma \left[ \frac{(T_w + 273)^2 + (T_g + 273)^2}{\left( \frac{1}{\varepsilon_w} + \frac{1}{\varepsilon_g} - 1 \right) (T_w + T_{gi} + 546)} \right] + 0.884 \left[ T_w - T_g + \frac{(P_w - P_{gi})(T_w + 273)}{2.689 \times 10^5 - P_w} \right]^{1/3} + 1.6273 \times 10^{-2} h_{cw} \frac{P_w - P_{gi}}{T_w - T_{gi}} \quad (3.68)$$

### 3.8 The Thermal Modelling of the Still

The energy balance equation of the three main components of the distiller unit is as follows

#### 3.8.1 Inner and Outer surface of the Glass Cover

When writing the energy balance equation for the glass cover it is mandatory to take the temperatures of the inner and the outer sides of the glass cover as different i.e.  $T_{gi} \neq T_{go}$ . This is the result of the thermal analyses by Tiwari *et al.*, (2002).

Therefore in this work that assumption is taken into consideration in setting the energy balance of the glass cover.

### 3.8.1.1 Inner side of the glass cover

For the inner side of the glass we can write

$$\tau_1 H_s + (\dot{q}_{rw} + \dot{q}_{cw} + \dot{q}_{ew}) = \left[ \frac{K_g}{L_g} \right] (T_{gi} - T_{go}) \quad (3.69)$$

Substituting the values of equations (3.44), (3.49) and (3.63) into (3.69) we obtain

$$\tau_1 H_s + h_2 (T_w - T_g) = \left[ \frac{K_g}{L_g} \right] (T_{gi} - T_{go}) \quad (3.70)$$

On simplifying equation (3.70) we can obtain

$$T_{gi} = \frac{\tau_1 H_s + h_2 T_w + (K_g / L_g) T_{go}}{h_2 + (K_g / L_g)} \quad (3.71)$$

### 3.8.1.2 Outer side of the glass cover

For the outer side of the glass the energy equation is

$$\left[ \frac{K_g}{L_g} \right] (T_{gi} - T_{go}) = \dot{q}_{rg} + \dot{q}_{cg} \quad (3.72)$$

By equation (3.4) we can write

$$\left[ \frac{K_g}{L_g} \right] (T_{gi} - T_{go}) = \dot{q}_g \quad (3.73)$$

Substituting equation (3.9) into (3.73) we get

$$\left[ \frac{K_g}{L_g} \right] (T_{gi} - T_{go}) = h_1 F_1 (T_{go} + T_a) \quad (3.74)$$

By substituting (3.71) into the LHS of (3.74) we get

$$\left[ \frac{K_g}{L_g} \right] (T_{gi} - T_{go}) = \frac{h_2 (K_g / L_g)}{h_2 + (K_g / L_g)} (T_w - T_{go}) + \frac{\tau_1 H_s (K_g / L_g)}{h_2 + (K_g / L_g)} \quad (3.75)$$

With equation (3.34) we can write

$$\left[ \frac{K_g}{L_g} \right] (T_{gi} - T_{go}) = U_{wo} (T_w - T_{go}) + h_k \tau_1 H_s \left( \frac{K_g}{L_g} \right) \quad (3.76)$$

where

$$h_k = \frac{(K_g/L_g)}{h_2 + (K_g/L_g)} \quad (3.77)$$

From equations (3.74) and (3.76) we can write

$$U_{wo}(T_{gi} - T_{go}) + h_k \tau_1 H_s \left( \frac{K_g}{L_g} \right) = h_1 F_1 (T_{go} - T_a) \quad (3.78)$$

Now from equations (3.70) and (3.74) the energy balance equation for the glass cover can be written as

$$\tau_1 H_s + h_2 (T_w - T_{gi}) = h_1 F_1 (T_{go} - T_a) \quad (3.79)$$

Simplifying equation (3.79) and solving for  $T_{go}$  we get

$$T_{go} = \frac{\tau_1 H_s h_k + U_{wo} T_w + F_1 h_1 T_a}{h_1 + U_{wo}} \quad (3.80)$$

### 3.8.2 The Basin liner

The rate of energy absorbed by the basin liner is equal to the rate of energy transferred to water and the rate lost by conduction through the bottom and sides. The equation for this balance is

$$\tau_3 H_s = \dot{q}_w + \dot{q}_b \quad (3.81)$$

On substituting the values of  $\dot{q}_w$  and  $\dot{q}_b$  from (3.60) and (3.36) in (3.81) we obtained

$$\tau_3 H_s = F_2 h_3 (T_b - T_w) + h_4 (T_b - T_a) \quad (3.82)$$

Simplifying equation (3.82) for  $T_b$  will give

$$T_b = \frac{\tau_3 H_s + F_2 h_3 T_w + h_4 T_a}{h_3 + h_4} \quad (3.83)$$

### 3.8.3 The Water Mass

The rate of energy absorbed and the rate of energy converted from the basin liner is equal to the rate of energy stored and rate of energy transferred to the glass cover.

$$\tau_2 H_s + \dot{q}_w + Q_u = M_w c_w \frac{dT_w}{dt} + (\dot{q}_{rw} + \dot{q}_{cw} + \dot{q}_{ew}) \quad (3.84)$$

Putting the values for  $\dot{q}$  s from (3.60), (3.44), (3.49) and (3.63) into (3.84) above, after simplification will give

$$\tau_2 H_s + h_3 F_2 (T_b - T_w) + Q_u = M_w c_w \frac{dT_w}{dt} + F_1 h_2 (T_w - T_{go}) \quad (3.85)$$

or

$$\tau_2 H_s + h_3 F_2 (T_b - T_w) + Q_u = (\rho l)_w c_w \frac{dT_w}{dt} + F_1 h_2 (T_w - T_{go}) \quad (3.86)$$

in terms of the water density and water depth.

The following assumptions have been made in setting up equation (3.85):

- There is no vapour leakage in the still;
- The temperatures of respectively the inner and the outer sides of the glass, the absorber and inside the insulator are supposed uniform;
- Water condensation on the cover is homogeneous and continuous;
- Lateral sides are at constant pressure (adiabatic);
- The temperature gradients along the glass cover thickness and water depth were assumed to be negligible;
- The heat capacity of the insulation is neglected;
- The physical properties of materials are considered constant.

Substituting the value for  $T_{go}$  and  $T_b$  from (3.70) and (3.83) respectively into (3.85) we get

$$Q_u + H_s \left[ \tau_3 \frac{h_3}{h_3 + h_4} + \tau_2 + \tau_1 \frac{h_2}{h_1 + U_{wo}} \right] = M_w c_w \frac{dT_w}{dt} + \left[ \frac{F_1 h_1 h_2}{h_1 + w_o} (T_w - T_{go}) \right] + \left[ \frac{F_2 h_3 h_4}{h_3 + h_4} (T_w - T_b) \right] \quad (3.87)$$

By substituting equations (3.35) and (3.39) into (3.87) above we get

$$Q_u + (\alpha\tau)_{eff} H_s = M_w c_w \frac{dT_w}{dt} + (U_t + U_b)(T_w - T_a) \quad (3.88)$$

where

$$(\alpha\tau)_{eff} = \left[ \tau_3 \frac{h_3}{h_3 + h_4} + \tau_2 + \tau_1 \frac{h_2}{h_1 + U_{wo}} \right] \quad (3.89)$$

In all active solar stills, additional thermal energy,  $Q_u$  is added to the distiller unit with the help of the collecting surface. This increases the temperature in the basin. To solve (3.88) therefore, the effect is considered. The useful energy per unit area from the flat plate collector is given by Sampathkumar *et al*, (2010) as

$$Q_u = NF_R [(\alpha\tau)_c H_{sc} - U_{Lc} (T_w - T_a)] \quad (3.90)$$

where N is the number of the collectors and  $F_R$  is heat removal factor. For a single plate collecting solar still as in this case,  $N = 1$ . By substituting (3.90) into (3.88) we get

$$F_R [(\alpha\tau)_c H_{sc} + U_{Lc} (T_w - T_a)] + (\alpha\tau)_{eff} H_s = M_w c_w \frac{dT_w}{dt} + (U_t + U_b + U_{sw})(T_w - T_a) \quad (3.91)$$

By substituting equation (3.43) into the above (3.91) we can write

$$F_R [(\alpha\tau)_c H_{sc} + U_{Lc} (T_w - T_a)] + (\alpha\tau)_{eff} H_s = M_w c_w \frac{dT_w}{dt} + [U_{Ls} + F_R U_{Lc}] (T_w - T_a) \quad (3.92)$$

Since the distiller unit is assumed to be leakage free  $F_R = 0$ . Therefore, we can write equation (3.92) as

$$(\alpha\tau)_{eff} H_s = M_w c_w \frac{dT_w}{dt} + U_L (T_w - T_a) \quad (3.93)$$

Dividing (3.73) by  $(M_w C_w)$  we get

$$\frac{dT_w}{dt} + \left[ \frac{U_L}{M_w c_w} \right] T_w = \left[ \frac{U_L}{M_w c_w} \right] T_a + \left[ \frac{(\alpha\tau)_{eff} H_s}{M_w c_w} \right] \quad (3.94)$$

Equation (3.94) is a first order differential equation in  $T_w$  which can be written as

$$\frac{dT_w}{dt} + aT_w = f(t) \quad (3.95)$$

where

$$a = \frac{U_L}{M_w c_w} \quad (3.96)$$

and  $f(t)$  is some functions of time given as

$$f(t) = \frac{(\alpha\tau)_{eff} H_s + U_L T_a}{M_w c_w} \quad (3.97)$$

$$(\alpha\tau)_{eff} = \tau_3 \frac{F_2 h_3}{F_2 h_3 + h_4} + \tau_2 + \tau_1 \frac{F_1 h_2}{h_1 + F_2 h_2} \quad (3.98)$$

$$U_L = U_i + U_b + U_{sw} \quad (3.99)$$

$$U_b = \frac{h_3 h_4}{h_3 + h_4} \quad (3.100)$$

$$U_i = \frac{F_1 h_1 h_2}{h_1 + F_1 h_2} \quad (3.101)$$

$$U_{sw} = \frac{F_2 h_3 h_4}{F_2 h_3 + h_4} \quad (3.102)$$

### 3.9 The Approximate Solution for the New Water Temperature, $T_w$

To obtain an approximate numerical solution of equation (3.95) we assume that:

- i the time interval  $\Delta t \sim 5$  minutes ( $0 < t < \Delta t$ ) is small in this case
- ii the function  $f(t)$  is constant, that is  $f(t) = \overline{f(t)}$  for the time interval  $\Delta t$  and
- iii  $a$  is also constant during the time interval  $\Delta t$

The value of  $h_l$  can be determined after considering the known values of  $T_w$  and  $T_g$  at  $t = 0$ , that is

$$T_w|_{t=0} = T_{w0} \quad \text{and} \quad T_g|_{t=0} = T_{g0} \quad (3.103)$$

Then solution to equation (3.95) can be derived as follows

$$T_w = \frac{\overline{f(t)}}{a} (1 - e^{-a\Delta t}) + T_{w0} e^{-a\Delta t} \quad (3.104)$$

where  $T_{w0}$  is the temperature of the basin water at  $t = 0$  and  $\overline{f(t)}$  is the average value of  $f(t)$  for the time interval  $\Delta t$ .

The average temperature of water  $T_w$  is given by

$$\overline{T_w} = \frac{1}{t} \int_0^t T_w dt \quad (3.105)$$

or

$$\overline{T_w} = \frac{\overline{f(t)}}{a} \left[ 1 - \frac{(1 - e^{-a\Delta t})}{a\Delta t} \right] + T_{w0} \frac{(1 - e^{-a\Delta t})}{a\Delta t} \quad (3.106)$$

The average glass temperature in terms of the water temperature can be obtained from equation (3.80) as

$$\overline{T_g} = \frac{\tau_1 H_s(t) + h_1 \overline{T_w} + h_1 \overline{T_a}}{h_1 + F_1 h_2} \quad (3.107)$$

From equation (3.106),  $T_w$  can be calculated as a function of time. At any time the heat flux due to the evaporation can be written as:

$$Q_{ew} = h_{ew}(T_w - T_{go}) \quad (3.108)$$

or

$$Q_{ew} = \frac{h_{ew}F_1h_2}{F_1h_2 + h_1}(T_w - T_a) \quad (3.109)$$

and the yield of evaporated water at the end of the 5<sup>th</sup> minute is given by

$$m = \frac{Q_{ew}}{\lambda} = \frac{h_{ew}(T_w - T_g)}{\lambda} \times 300 \times A_b \quad (3.110)$$

while the cumulative yield is

$$M = \sum_{i=1}^{288} m \quad (3.111)$$

After obtaining the timely yield, the value of  $M_w C_w$  for the next interval reduces by  $mC$  as such it becomes

$$M_w c_w - m c_w \quad (3.112)$$

The instantaneous efficiency,  $\eta_i$  of a solar still, defined as the ratio of the energy used for water production to the total solar radiation rate is given by:

$$\eta_i = \frac{Q_{ew} A_b}{H_s A_b} = \frac{Q_{ew}}{H_s} = \frac{h_{ew}(T_w - T_g)}{H_s} \quad (3.113)$$

and from equation (3.109) we can write

$$\eta_i = \frac{h_{ew}F_1h_2}{h_1 + F_1h_2}(T_w - T_a) \quad (3.114)$$

The above equation can be rewritten by substituting the value of  $T_w$  from equation (3.106) as

$$\eta = \frac{F_1 h_{ew} h_2}{h_1 + F_1 h_2} \frac{1}{U_L} \times \left[ (\alpha \tau)_{eff} (1 - e^{-a\Delta t}) + U_L \frac{(T_{w0} - T_a)}{H_s} e^{-a\Delta t} \right] \quad (3.115)$$

As it is seen, the efficiency,  $\eta$ , is also a function of time. The variation of the instantaneous efficiency,  $\eta$  with  $\frac{T_{w0} - T_a}{H_s}$  can be shown for the typical climatic conditions of the place of research (**Yola**) and the design parameters. As can be seen from the equation (3.115), the slope is positive unlike that of the flat plate collectors. This is due to the fact that efficiency,  $\eta$  in this case is higher for the maximum top loss coefficient,  $U_t$  which includes  $h_{ew}$  whereas it is minimum for higher  $\eta$  in the case of the flat plate collector. The non linear behaviour is due to the temperature dependency of  $h_{ew}$ .

### 3.10 Steps in Solving the Theoretical Model

Since  $T_w$ ,  $T_g$ ,  $T_a$ ,  $H_s$ ,  $m$ ,  $\eta$  and  $M_w$  in the basin vary with time, a numerical approach was used for their calculations. In this work, the time interval  $\Delta t$  was taken as 5 minutes. The following procedure was used for the computations:

1. The heat transfer coefficients were calculated using the initial values of  $T_w$ ,  $T_g$ , solar still specifications and other climatic parameters.
2. Knowing the heat transfer coefficients,  $T_w$ ,  $T_g$ , and as a result  $T_a$  at the end of the first time interval  $\Delta t$  were calculated using equations (3.82) and (3.85).
3. Using the new values of  $T_w$ ,  $T_g$  and  $T_a$ , the heat transfer coefficients were recalculated and step 2 repeated for another time interval, so on.
4. During each time interval,  $T_w$ ,  $T_g$ ,  $T_a$ , and also the heat transfer coefficients and climatic parameters were assumed to be constant and so the rate of water evaporation was calculated for each time interval; and as a result the total amount of fresh water production was calculated for that time interval.
5. For each time interval,  $\Delta t$  the solar efficiency  $\eta$  was calculated.
6. For each time interval the amount of water in the basin was considered as the initial amount of water fed to the still minus the total amount of evaporated water up to that time.

A flow chart for the numerical procedures is depicted in fig. 3.3.

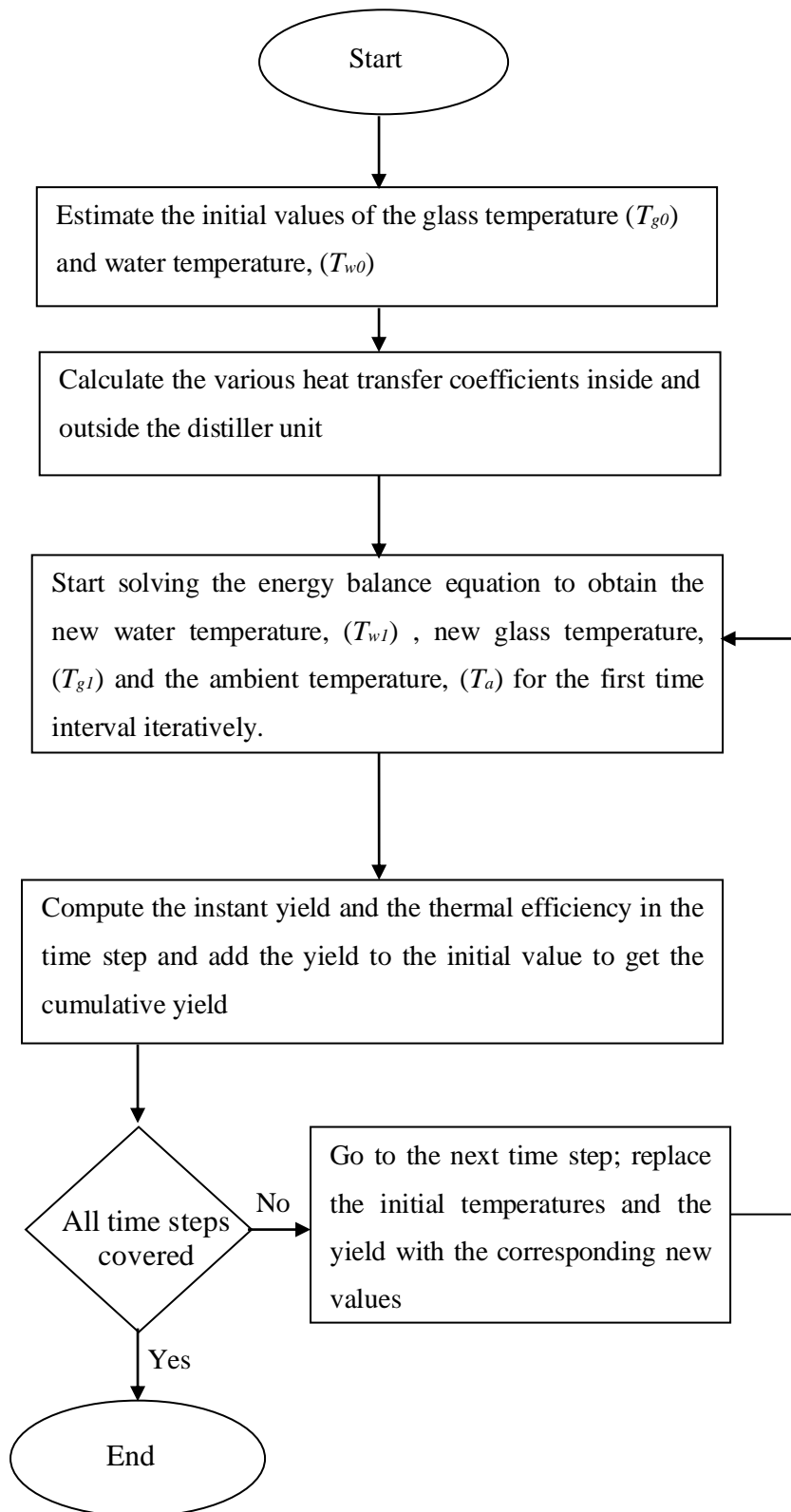


**Figure 3.3: Flow Chart for Computing the Distiller Yield and Thermal Efficiency.**

### **3.11 Materials and Construction**

#### **3.11.1 *Materials for the Experiment***

The materials used for this research work were obtained from the Department of Physics, Modibbo Adama University of Technology, Yola using the meteorological unit set up by Nigerian Environmental Climatic Observing Program (NECOP) Nigeria in the Department. The Unit was linked up to its main station at University of Nigeria Nsukka through a wireless network along with ten (10) other units sepreads in the country cutting across the six geopolitical locations. The data logger used in this research was installed in the NECOP Yola data station. The following materials were used:

- (i) A computer set with a workable programme especially Excel and a printer for the data generation/analysis.
- (ii) A conventional basin type solar still constructed so as to test the validity of the developed model.
- (iii) A data logger mounted in an open space behind the Physics Department block for recording the data.

The data logger is then linked with the computer PC either through an MTN modem which obtained the data using the net or by using a USB data cable directly for downloading, analyses, and comparison.

#### **3.11.2 *Construction Materials***

The materials used for the construction of the distiller unit includes the following: Aluminium sheet, Plywood, marker pen, Cotton wool, Top bond gum, Top bond glue, Black paint, Leather fore maker, Iron road, Soldering sticks, Flank wood Plastic water pipes, Plastic water tap, Plastic bucket, Silver plated ruler, Flash band Thermocouples probes, Digital multi-meters, Glass sheet and Measuring cylinder

#### **3.11.3 *The Construction Procedure***

The construction of the still was an interesting experience, and the design features consist of a basin (1.0 m<sup>2</sup> basin area) of 50 cm height made of the Aluminium metal which was coated with a black paint. The metal box is sloped at one side at an angle of 9.23° to the horizontal. It was then inserted into a 5 mm lagged (with cotton

wool), larger plywood box. The top was covered with a transparent glass. The whole assembly was covered externally with a leather fore maker for protection against the influence of rain and external moisture. The slopping pane of glass, supported by the appropriate frame which covers the upper part of the basin was sealed tightly with a water proof cellotape to minimise the vapour leakage.

The still was fed with a saline/ dirty / unclean water from the water tank at a shallow depth through the back upper tap. A distillate trough ran along the lower edge of the glass pane to collect the distillate and channel it out through the out let pipe to the measuring cylinder placed on top of a weighing balance which measured and weigh the distillate. The weighing balance was placed on a stool (not shown in the figure), below the out let pipe. The refilling tube for refilling the basin was located near the upper edge of the still, and a level controller also served as a drain to carry away the brine/ brackish water located near the bottom of the still. The sectional view of the still is shown in Fig. (3.4).

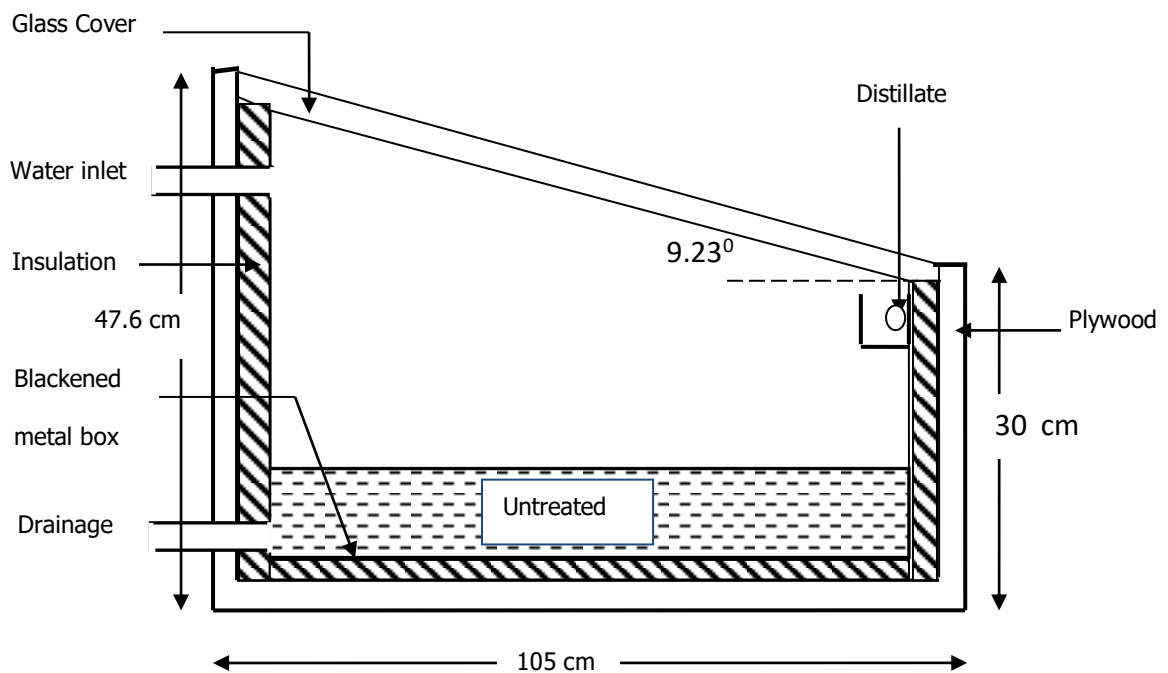


**Figure 3.4: Cross-sectional view of the distiller unit (not mounted)**

The whole assembly was mounted on a table (1m above the ground level) in a shadowless area at the back of the Physics Department MAUTECH building, and it was oriented so that the slope of the still runs in East-West direction. The refilling bucket (tank) was placed on top of the upper table 1.5 m above the ground. It provides

shade to the data recording table which was right under it at a level of 1m from the ground. The sloping glass cover slants towards the equator for maximum solar radiation. The schematic diagram of the assembly is shown in Figure (3.5).

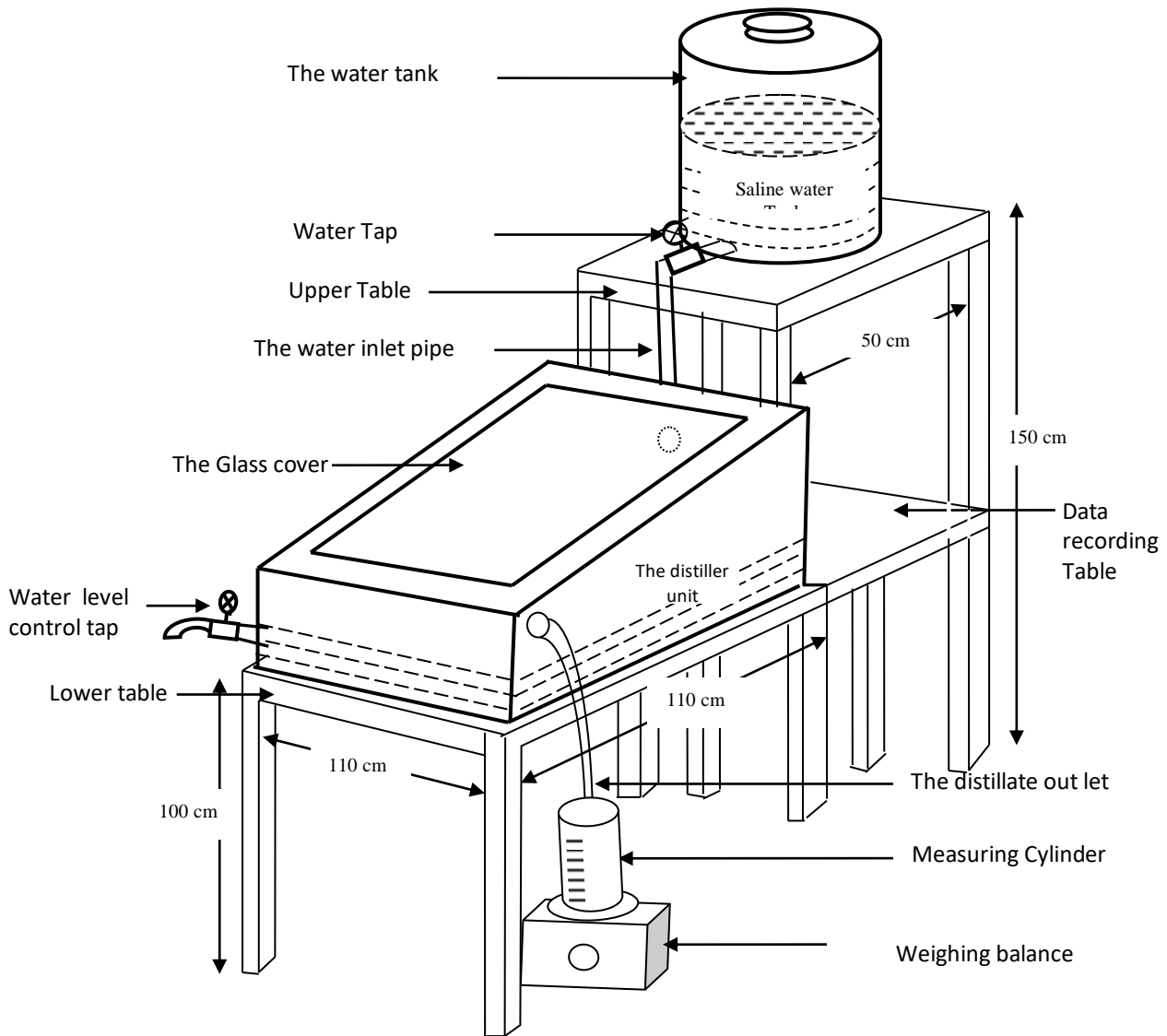


**Figure 3.5: The experimental set up of the solar still to be used (Mounted)**

### **3.11.4 The Method of Experimental Observation**

To obtain the data from the Solar distiller, water was fed into the basin to a specified depth in the morning and the amount of the collected distilled water, ambient temperature, glass temperature and water temperatures were measured weighed and recorded after every 30 minutes from 7 a.m. to 7 a.m. the following

morning. The solar insolation,  $H_s$ , wind velocity,  $v$ , and the relative humidity, R.H. were obtained from the records of the Logger in the NECOP Centre inside the Modibbo Adama University of Technology, Yola Campus.

### **3.12 Operational Framework**

The still was constructed to suite operation in Yola North-Eastern Nigeria with the aim of producing the maximum yield (about 3.6 litres) of distilled water a day. Therefore, the framework within which the solar distiller is operated is that which corresponds to the optimum results that can be attained to by using the values of the climatical data (e.g. the latitude, average temperature, average wind speed, average solar insolation etc.) obtained in the place of research, Yola.

### **3.13 Method of Data Collection**

#### **3.13.1 Theoretical Data Generation**

The steps involved in obtaining the results of the theoretical model were explained in section 3.10. A Microsoft Excel page formula bar was used for the theoretical data generation. The results are presented for a complete day each (i) in dry season (12<sup>th</sup> November, 2009) and (ii) wet season (1<sup>st</sup> August, 2009) as shown in Tables (4.5a) and (4.5b).

#### **3.13.2 Data Acquisition System**

The data acquisition system comprises of a NECOP data logger with ten (10) inputs for sensing ten (10) different environmental parameters at a time. These are:-

(i) Time of the day (min) (ii) Solar insolation,  $H_s$  ( $W/m^2$ ) (iii) Air Temperature, ( $^{\circ}C$ ) (iv) Relative Humidity, R.H (%) (v) Wind speed,  $v$  (m/s) (vi) Wind Direction, (degrees) (vii) Soil Temperature ( $^{\circ}C$ ) (viii) Rain gauge (mm) (ix) Rain rate (mm/hrs) (x) Atmospheric pressure (Bars).

Four out of these were used in this research viz: (i) Solar insolation (ii) wind speed (iii) air temperature and (iv) Relative humidity. The logger is mounted in an open environment together with a micro computer system with a monitor, printer and disc/USB input facility. The data logger and the computer set were interfaced. This

method has become the established means of configuring laboratory-scale data collection system (Ekechukwu, 1997).

The schematic diagram of the data acquisition system used in this research for the theoretical data generation are as shown in Figure (3.6).

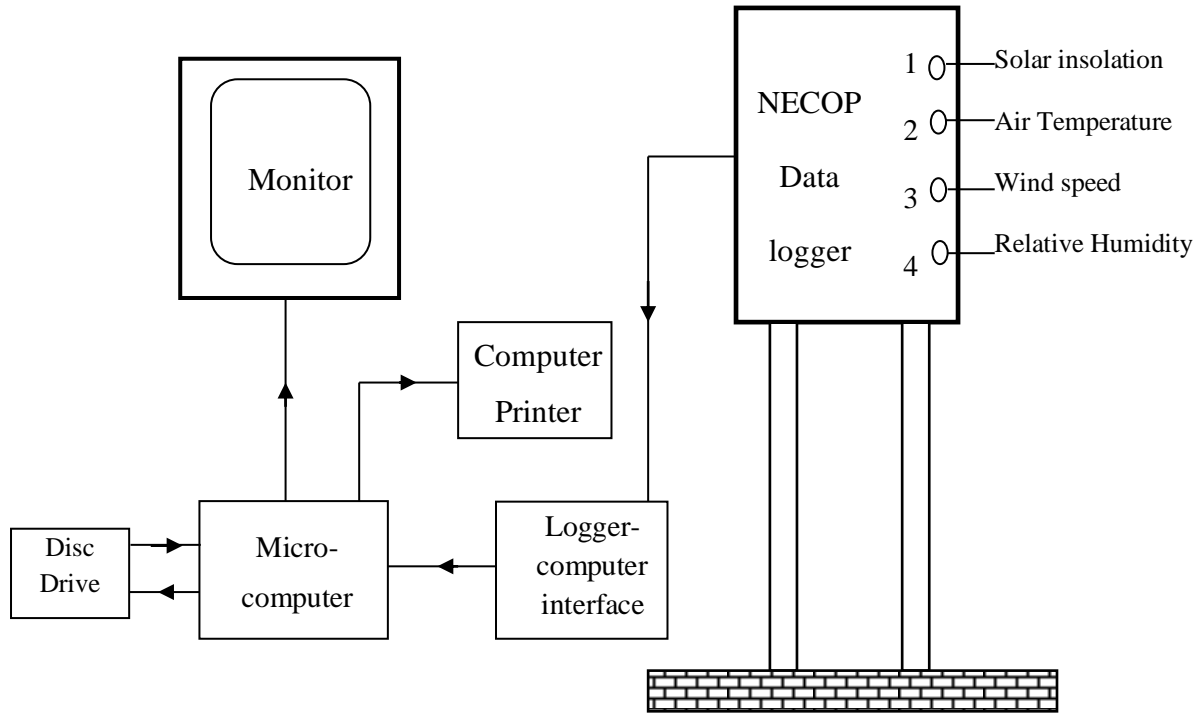


*Figure 3.6: Schematic Diagram of the data acquisition system*

### 3.13.3 Data Aquisition Program

The data acquisition and manipulation software developed for this study are of two major categories Viz:-

- (i) The main data acquisition program
- (ii) The data reduction, analysis and presentation programs

**Data acquisition program:** The main data acquisition program was used to perform the following:

- Continually calculating real time
- Reading all the sensors when required
- Applying conversion factors (and zero offsets where necessary) to all sensor readings in order to give the appropriate values

- Storing these parametric data on the logger and USB/CD disc
- Displays these recorded data on the computer monitor

**Data Reduction:** The data reduction and presentation was used to perform the following

- Convert and displays the data of any specified sensor on the monitor in tabular form on the Microsoft excel page
- Displays the previous readings of any specified sensor on the monitor

#### **3.13.4 Sensors**

The detail of all sensors used in the data acquisition for theoretical modelling are shown in table 3.4. With the exception of the distillate guage, which measures the amount of the distillate collected over a time and the temperature/humidity sensors, all the sensors give output in milli-volts, mV. The temperature/humidity sensors give output in milli-amperes, mA that are directly proportional to temperature or relative humidity respectively. The NECOP data logger and the microcomputer performed the appropriate conversions on the mV sensor outputs.

**Table 3.4: Sensors used in the Data Acquisition and Generation (Modelling)**  
**(Source: (i) NECOP Data Center (ii) Equipments Purchase Flare)**

S/N	Sensor type	Parameter measured	No. required	Units of data output	Accuracy (% error)
1	Thermocouple	Various temperature	3	°C	±2°C
2	Mercury in glass thermometer	Ambient temperature	1	°C	±2%
3	Solar cell	Solar insolation	1	wm <sup>-2</sup>	±2%
4	Pyranometer	Solar insolation	1	wm <sup>-2</sup>	±2%
5	Anemometer	Wind speed	1	ms <sup>-1</sup>	±1%
6	Measuring cylinder	Daily distillate	1	cm <sup>3</sup>	±0.5%
7	NECOP data logger	4 sensors at a time	1	required conversion	-
8	Humidity	Air humidity	1	%	±2%
9	Wind vane	Wind direction	1	Degrees	±2%
10	Weighing balance	Total mass of the water collected	1	Grames	±2%

## **CHAPTER FOUR**

### **RESULTS**

#### **4.1 Introduction**

The chapter presents the results obtained in this research, which include the theoretical and experimental data and their graphical plots. The water quality results as well as the result of comparison between the constructed distiller and a standard electronic distiller are presented as well. The result variation of the various distiller components with the climatic conditions of the study area and their effects on the distiller output are presented.

#### **4.2 Results**

##### ***4.2.1 The Water Quality Test Results***

The results of the quality of the distillate produced were presented in Table (4.1). Some contaminated water taken from four (4) different wards of the research area were introduced into the distiller and the output was tested and the results presented. Also, the quality of the water produced was compared with that produced by an electronic distiller as presented in table (4.2).

**Table 4.1: Results of the Water Quality Test**

<b>Parameter Tested</b>	<b>Location</b>	<b>Input Water (from the Source )</b>	<b>Output Water (from the Distiller)</b>
<b>pH</b>	<b>FUTY Campus</b>	7.1	7.0
	<b>Girei town</b>	7.2	7.1
	<b>Vonoklang</b>	7.8	7.1
	<b>Sabongari</b>	7.6	7.1
<b>Water Hardness (CaCO<sub>3</sub>) (mg/l)</b>	<b>FUTY Campus</b>	250	0.0
	<b>Girei town</b>	260	0.0
	<b>Vonoklang</b>	260	0.0
	<b>Sabongari</b>	260	0.0
<b>Aerobic Bacterial Count (cfu/ml)</b>	<b>FUTY Campus</b>	2.1 x 10 <sup>4</sup>	0.0
	<b>Girei town</b>	3.0 x 10 <sup>4</sup>	0.0
	<b>Vonoklang</b>	3.0 x 10 <sup>4</sup>	0.0
	<b>Sabongari</b>	2.3 x 10 <sup>4</sup>	0.0
<b>Distribution of coli form bacteria (%)</b>	<b>FUTY Campus</b>	100%	0.0
	<b>Girei town</b>	100%	0.0
	<b>Vonklang</b>	100%	0.0
	<b>Sabongari</b>	100%	0.0

**Table 4.2: Comparison between the Results of the Water Quality Test of the Constructed Distiller Unit and that of the Standard Electronic Distiller**

<b>Parameter Tested</b>	<b>Units</b>	<b>Sample before distillation</b>	<b>Distillate from the Constructed Distiller</b>	<b>Distillate from the Electronic Distiller</b>	<b>Max. WHO Standard</b>
<b>pH</b>	-	7.5	7.1	7.0	6.5-8.5
<b>Taste</b>	-	Tasteless	Tasteless	Tasteless	NGV
<b>Turbidity</b>	NTU	3.0	2.8	2.7	5.0
<b>Temperature</b>	°C	31.5	31.5	31.5	Ambient
<b>Odour</b>	-	no objection	no objection	no objection	NGV
<b>Conductivity</b>	HS/cm	88	0.0	0.0	0.0
<b>Total Hardness (CaCO<sub>3</sub>)</b>	mg/l	260	0.0	0.0	NGV
<b>Total Iron (Fe) content</b>	mg/l	1.04	0.0	0.0	0.0
<b>Aerobic Bacterial Count</b>	cfu/ml	2.1 x 10 <sup>4</sup>	0.0	0.0	0.0
<b>Distribution of coli form bacteria</b>	(%)	100%	0.0	0.0	0.0

**Note** NTU = Nephelometric Turbidity Unit

NGV = No Guide Value

#### 4.2.2 The Theoretical Modelling Results

The theoretical results of the cumulative distiller yield, the water temperatures, glass cover temperatures and the efficiency of the solar still were obtained using equations (3.87), (3.90), (3.91) and (3.93) respectively taking the distiller specifications (Table 4.3) into consideration. The results were generated at an assumed initial water depth of 1.0 cm, the initial glass/water temperatures of 26°C/27°C on the 12<sup>th</sup> November, 2009 (a dry season period) and 19°C/20°C on the 1<sup>st</sup> August 2009 (a wet season period) respectively. The results are as presented in Tables (4.4a) and (4.4b). Fig. 4.3 displays part of the processed result on November 12, 2009.

**Table 4.3: The Distiller Specifications**

<b>Parameter</b>	<b>Value</b>
<b>A : Basin Area</b>	1.0000 m <sup>2</sup>
<b>F<sub>1</sub> : Top correction factor</b>	1.0131
<b>F<sub>2</sub> : Side wall correction factor</b>	0.3870
<b>F<sub>3</sub> : Still correction factor</b>	1.4001
$\alpha_g$	0.0000
$\alpha_w$	0.2000
$\alpha_b$	0.0700
$R_g$	0.0500
$R_w$	0.0500
$R_{gr}$	0.2000
$\varepsilon_g$	0.9000
$\varepsilon_w$	0.9000
$h_3 = h_w$	100 W/m <sup>2</sup> °C
$k_i$ : (cotton wool)	0.0400 W/m°C
$L_i$	0.0050 m
$l$	0.0100 m
$U_{wo}$	1.2030 Wm <sup>-2</sup> K <sup>-1</sup>
$U_{sw}$	0.5000 Wm <sup>-2</sup> K <sup>-1</sup>